disease, kidney disease, chronic hepatic disease, cancer, or diabetes mellitus. The patients were diagnosed on the basis of DSM-IV criteria, information from medical records and a clinical interview. All patients were stable and/or partially remitted at the time of MR measurement and neuropsychological tests.

According to genotypes, each group (control and schizophrenia) was categorized into three groups; the homozygous Val-COMT group (control: n = 38, two were left-handed, schizophrenia: n = 19, one was left-handed), the Val/Met-COMT group (control: n = 25, three were left-handed, schizophrenia: n = 22, all were right-handed) and the remaining homozygous Met-COMT group (control: n = 13, all were right-handed, schizophrenia: n = 6, all were right-handed). Because of the small number of subjects with homozygous Met-COMT, the Val/Met-COMT and homozygous Met-COMT groups were combined and treated as one group, the Met-COMT carriers. Table 1 shows the characteristics of each group. All groups were of comparable age, gender (χ^2 test, df = 3, P = 0.38) and handedness (χ^2-test, df = 3, P = 0.53). No genotype effects and genotype-diagnosis interaction effects were found in years of education, scores of full scale Intelligence Quotient (IQ) and scores of premorbid IQ [Japanese version of National Adult Reading Test (JART) score], however, patients who had fewer years of education ($P < 0.0001$), had lower scores of both full scale IQ and JART ($P < 0.001$). The duration of illness, medication and hospitalization, the age at disease onset and drug dose (chlorpromazine equivalent) of those homozygous for the Val-COMT did not differ from the Met-COMT carriers.

SNP genotyping

Venous blood was drawn from subjects and genomic DNA was extracted from whole blood according to the standard procedures. The Val158Met polymorphism of the COMT gene (dbSNP accession: rs4680) was genotyped using the TaqMan 5′-exonuclease allelic discrimination assay, described previously (Hashimoto *et al.*, 2004, 2005). Briefly, primers and probes for detection of the SNP are: forward primer 5′-GACTGTGCCGCCATCAC-3′, reverse primer 5′-CAGGCATGCACACCTTGTC-3′, probe 1 5′-VIC-TTTCGCTG-GCGTGAAG-MGB-3′ and probe 2 5′-FAM-CGCTGGCATGAAG-MGB-3′. PCR cycling conditions were: at 95°C for 10 min, 50 cycles of 92°C for 15 s and 60°C for 1 min.

MRI procedures

All MR studies were performed on a 1.5 tesla Siemens Magnetom Vision plus system. A three dimensional (3D) volumetric acquisition of a T_1-weighted gradient echo sequence produced a gapless series of thin sagittal sections using an MPRage sequence (TE/TR, 4.4/11.4 ms; flip angle, 15°; acquisition matrix, 256 × 256; 1 NEX, field of view, 31.5 cm; slice thickness, 1.23 mm).

Image analysis (TBM)

The basic principle of TBM is to analyse the local deformations of an image and to infer local differences in brain structure. In TBM, MRI scans of individual subjects are mapped to a template image with three-dimensional (3D) non-linear normalization routines. Local deformations were estimated by a univariate Jacobian approach. The basic principle of TBM is the same as a method used in a previous report described as deformation-based morphometry (Gaser *et al.*, 2001). Firstly, inhomogeneities in MR images were corrected using a bias correction function in statistical parametric mapping (SPM2), then the corrected image was scalp-edited by masking with a probability image of brain tissue obtained from each image using a segmentation function in SPM2. Using a linear normalization algorithm in SPM2, all brains were resized to a voxel size of 1.5 mm and adjusted for orientation and overall width, length and height (Fig. 1A). Therefore, brains were transformed to the anatomical space of a template brain whose space is based on Talairach space (Talairach and Tournoux, 1988). Subsequent non-linear normalization introduced local deformations to each brain to match it to the same scalp-edited template brain (Fig. 1C). The non-linear transformation was done using the high-dimension-warping algorithm (Ashburner and Friston, 2004). After the high dimensional warping, each image (Fig. 1B) looks similar to the template (Fig. 1C). Figure 2 demonstrated a mean MR image of 76 controls (left) and a mean MR image of 47 schizophrenics after high dimensional warping (Fig. 2). We obtained 3D deformation fields for every brain (Fig. 1D). Each of these 3D deformation fields consists of displacement vectors for every voxel, which describe the 3D displacement needed to locally deform the brain to match it to the template. We calculated the Jacobian determinants to obtain voxel by voxel parametric maps of local volume change relative to the template brain (Fig. 1E). The local Jacobian determinant is a parameter commonly used in continuum mechanics (Gurtin, 1987), which characterizes volume changes, such as local shrinkage or enlargement caused by warping. The parametric maps of Jacobian determinants were analysed using SPM2, which implements a 'general linear model'. To test hypotheses about regional population effects and interaction, data were analysed by an analysis of covariance (ANCOVA) without global normalization. There was no significant difference in age among the four groups, however, patients with schizophrenia, particularly those homozygous for the Val-COMT allele, were older than controls. Therefore, we treated age and years of education and scores of JART as nuisance variables. Since TBM explores the entire brain (grey matter, CSF space and white matter) at once, the search volume of TBM has a large number of voxels and since our interest was in morphological changes in the grey matter and CSF space, we excluded white matter tissue from analyses by using an explicit mask (Fig. 1F). We used $P < 0.001$, corrected for multiple comparisons with false discovery rate (FDR) <0.05 as a statistical threshold. The resulting sets of t values constituted the statistical parametric maps {SPM (t)}. Firstly, we estimated the main effects, the genotype effect in total subjects (the Val/Val-COMT versus the Met-COMT carriers) and the diagnostic effect (schizophrenia versus controls) and then the genotype-diagnosis interaction effect was estimated. Furthermore, the effects of genotypes in each group (controls carrying the Val/Val-COMT gene versus controls carrying the Met-COMT gene and schizophrenics carrying the Val/Val-COMT gene versus schizophrenics carrying the Met-COMT gene) were estimated within the ANCOVA design matrix. Anatomical localization accorded both to MNI coordinates and Talairach coordinates obtained from M. Brett's transformations (www.mrc-cbu.cam.ac.uk/Imaging/mnispace.html) and are presented as Talairach coordinates (Talairach and Tournoux, 1988). Since previous studies have demonstrated the association between the Val158Met polymorphism and the dorsolateral PFC (DLPFC), we applied an additional hypothesis-driven region of interest (ROI) method to test regional population effects in the DLPFC. For this ROI analysis, we used the Wake Forest University PickAtlas (Maldjian *et al.*, 2003) within the ANCOVA design matrix for SPM analysis. We set $P < 0.05$ (uncorrected) with a small volume correction ($P < 0.05$ within the ROI) to assess grey matter volume changes in the DLPFC (Brodmann area 46, 9 and 8).

Table 1 Subject characteristics

	Control Val/Val	Met carriers	Schizophrenia Val/Val	Met carriers	Diagnosis F (P)	Genotype F (P)*	Genotype by diagnosis F (P)
Number of subjects	38	38	19	28			
Gender (M/F)	16 out of 22	14 out of 24	11 out of 8	13 out of 15			
Handedness (R/L)	36 out of 2	35 out of 3	18 out of 1	28 out of 0			
Age (years)	41.47 (13.42)	39.26 (10.6)	45.98 (15.29)	43.05 (10.57)	3.633 (0.059)	1.7 (0.195)	0.21 (0.647)
Education (years)	17 (3.16)	16.06 (2.57)	12.67 (2.43)	13.33 (3.31)	30.855 (<0.0001)	0.047 (0.828)	1.61 (0.208)
Full scale IQ (WAIS-R)	113.42 (12.05)	108.93 (13.58)	80.69 (17.68)	88.958 (22.08)	57.9 (<0.001)	0.29 (0.59)	3.41 (0.068)
JART	78.8 (10.45)	75.42 (13.65)	54.69 (20.74)	62.25 (27.06)	23.366 (<0.001)	0.292 (0.59)	2.014 (0.159)
Wechsler Memory Scale—Revised							
Verbal memory	111.78 (15.001)	111.061 (12.89)	78.0 (21.623)	81.33 (18.57)	86.93 (<0.001)	0.147 (0.702)	0.354 (0.553)
Visual memory	112.1 (8.51)	106.55 (11.99)	74.78 (24.32)	83.29 (20.613)	85.51 (<0.001)	0.204 (0.65)	4.605 (0.03)
General memory	113.31 (13.92)	110.85 (12.22)	74.43 (21.3)	79.33 (19.14)	111.93 (<0.001)	0.135 (0.715)	1.226 (0.27)
Attention/concentration	104.47 (13.25)	102.94 (16.51)	87.79 (19.09)	92.54 (17.38)	16.08 (0.001)	0.228 (0.634)	0.866 (0.14)
Delayed recall	111.88 (15.46)	112.48 (10.08)	77.07 (20.92)	81.21 (19.19)	99.74 (<0.001)	0.52 (0.475)	0.284 (0.59)
WCST (preservative error)	2.5 (3.89)	3.14 (3.90)	12.08 (11.54)	8.52 (10.63)	24.5 (<0.0001)	0.93 (0.34)	1.93 (0.17)
Digit span	11.12 (3.25)	10.77 (3.34)	7.83 (3.93)	9.09 (2.74)	12.165 (0.0007)	0.415 (0.52)	1.28 (0.261)
Onset age			25.38 (10.34)	23.74 (7.992)		0.52	
Duration of illness (years)			19.86 (14.93)	18.84 (9.8)		0.77	
Duration of hospitalization (months)			66 (153.41)	59.59 (91.18)		0.86	
Duration of medication (years)			12.86 (14.21)	16.4 (9.89)		0.29	
Drug dose of typical antipyschotic drugs (mg/day, chlorpromazine equivalent)			617.9 (720.18)	700.38 (752.67)		0.69	
Drug dose of atypical antipyschotic drugs (mg/day, chlorpromazine equivalent)			282.3 (428.29)	340.23 (482.19)		0.66	

Mean (standard deviation); WAIS-R = Wechsler Adult Intelligence Scale—Revised; JART = Japanese version of National Adult Reading Test; WCST = Wisconsin Card Sorting Test.

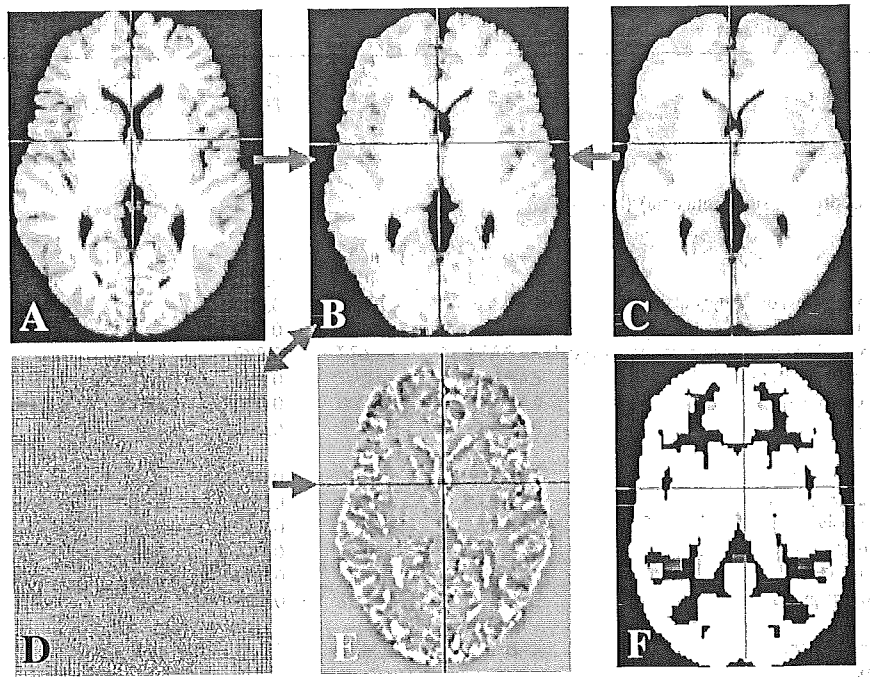

Fig. 1 Steps of analysis for tensor-based morphometry. An example is shown for a single subject in one axial slice. The single object brain (**A**) has been corrected for orientation and overall size to the template brain (**C**). Non-linear spatial normalization removes most of the anatomical differences between the two brains by introducing local deformations to the object brain, which then (**B**) looks as similar as possible to the template. Image (**D**) shows the deformations applied to the object brain by a deformed grid. Statistical analysis can be done univariate using the local Jacobian determinant as a derivative of the field (**E**). An explicit mask image (**F**) was used to explore morphology in the grey matter and CSF space.

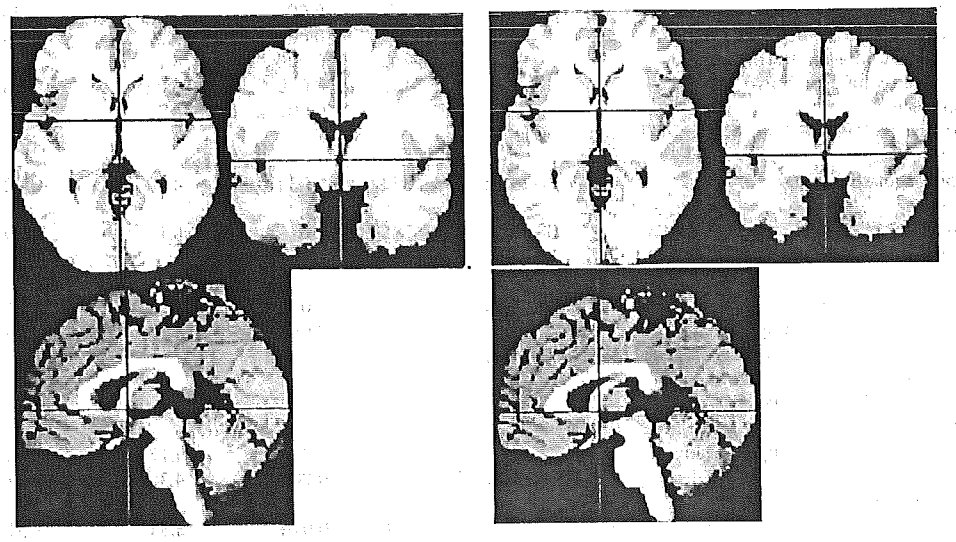

Fig. 2 Mean images after high dimensional warping control subjects and schizophrenics. *Left*: The mean image of warped MR images obtained from 76 controls. Even after averaging, the mean image is not blurred. *Right*: The mean image of warped MR images obtained from 47 schizophrenics. The mean image of schizophrenic looks similar to that of controls.

Results

Behavioural data

Patients had a lower full scale IQ, measured by the Wechsler Adult Intelligence Scale—Revised, than controls. They also had a lower expected premorbid IQ measured by a JART, lower scores of Wechsler Memory Scale—Revised and demonstrated poorer performance of working memory measures such as the number of preservative errors in the WCST and digit span (Table 1). No genotype or genotype-diagnosis interaction effects were found in working memory measures

Table 2 Results of image analyses

Anatomical regions	Brodmann area	Cluster size	Corrected P FDR	*T*-value (voxel level)	Talairach coordinates		
					x	*y*	*z*
Main effects							
Diagnosis effects (control > schizophrenia) (Fig. 3)							
Limbic system							
R insula	BA13	4682	0.000	6.41	33	11	−2
L insula	BA13	4017	0.000	8.81	−33	11	4
R parahippocampal gyrus, amygdala-uncus	BA36	4682	0.000	7.32	30	1	−17
R parahippocampal gyrus	BA36	186	0.000	5.04	30	−41	−8
L parahippocampal gyrus, hippocampus-amygdala	BA34/36	637	0.000	5.46	−20	−41	−8
R anterior cingulate cortex	BA32	147	0.000	4.9	9	33	20
L anterior cingulate cortex	BA32	200	0.000	4.63	−11	32	20
L cingulate gyrus	BA32	275	0.001	4.2	−12	−16	39
Prefrontal cortex							
R inferior frontal gyrus	BA47,11	145	0.000	4.99	27	28	−11
R superior frontal gyrus	BA8/9	1889	0.000	6.08	12	43	39
L medial frontal gyrus	BA9	1333	0.000	5.13	−8	47	19
L inferior frontal gyrus	BA45	141	0.000	4.55	−44	23	15
L middle frontal gyrus	BA8	482	0.000	4.44	−30	24	43
L superior frontal gyrus	BA8	482	0.000	4.39	−35	17	51
Premotor area							
R dorsal premotor area	BA6	429	0.000	4.37	41	13	45
Temporal cortex							
R superior temporal gyrus	BA22	806	0.000	5.04	47	−23	−1
R middle temporal gyrus	BA21	806	0.000	4.87	56	−15	−3
L superior temporal gyrus	BA38	4017	0.000	7	−36	1	−17
Central grey matter							
L thalamus		4017	0.000	7.26	−15	−17	2
Diagnosis effects (control < schizophrenia) (Fig. 4)							
L sylvian fissure		621	0.000	6.7	−45	17	−3
R sylvian fissure		774	0.000	6.59	44	17	−8
Lateral ventricle (anterior horn)		279	0.000	5.27	−5	21	4
Lateral ventricle (L inferior horn)		248	0.000	6.18	−41	−30	−10
Lateral ventricle (R inferior horn)		137	0.000	5.02	36	−40	−1
Interhemisphrenic fissure		154	0.000	5.28	3	55	−12
Genotype effects (Val/Val-COMT < Met-COMT carriers) (Fig. 5)							
Limbic system							
L anterior cingulate cortex	BA24/25	334	0.033	4.29	−8	17	−13
Temporal cortex							
R middle temporal gyrus	BA21	285	0.016	5.10	59	−3	−14
Genotype-diagnosis interaction effects (Fig. 6)							
Limbic system							
L anterior cingulate gyrus	BA24/25/32	264	0.044	3.77	−6	25	−6
L parahippocampal gyrus, amygdala-uncus	BA34	219	0.048	3.74	−24	−6	−14
The effects of polymorphism in control group (no significant difference)							
The effects of polymorphism in schizophrenia							
Val/Val-COMT < Val/Met, Met/Met-COMT (Fig. 7)							
Limbic system							
L parahippocampal gyrus, amygdala-uncus	BA28	81	0.010	4.17	−26	2	−22
L anterior cingulate cortex	BA24/25/32	263	0.007	4.38	−7	20	−8
Central grey matter							
L thalamus		91	0.014	3.94	−21	−28	6

and IQ, however, a significant genotype-by-diagnosis interaction effect was found in a visual memory measure (F = 4.605, df = 1, P = 0.03) (Table 1). However, a *post hoc t*-test (Bonferroni test) demonstrated no genotype effect in each diagnostic category (control: P = 0.15, schizophrenia: P = 0.11).

Morphological changes in schizophrenia (diagnosis effects)

In comparison with controls, patients with schizophrenia demonstrated a significant reduction of volumes in multiple brain areas, such as the limbic and paralimbic systems, neocortical areas and the subcortical regions (Table 2 and Fig. 3).

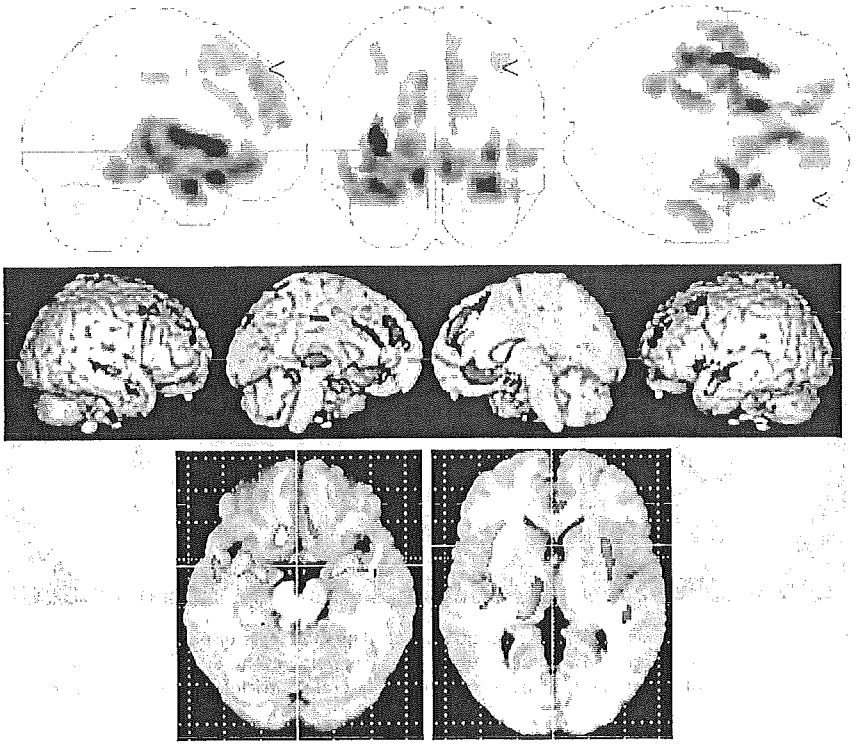

Fig. 3 Decreased volumes in schizophrenics ($n = 47$) as compared to controls ($n = 76$). *Top*: The SPM {t} is displayed in a standard format as a maximum-intensity projection (MIP) viewed from the right, the back and the top of the brain. The anatomical space corresponds to the atlas of Talairach and Tournoux. Representation in stereotaxic space of regions with significant reduction of volume in schizophrenia was demonstrated. Schizophrenics demonstrated a significant reduction of volumes in the multiple brain areas, such as the limbic and paralimbic systems, neocortical areas and the subcortical regions. *Middle*: The SPM {t} is rendered onto T_1-weighted MR images. *Bottom*: The SPM {t} is displayed onto axial T_1-weighted MR images. A significantly decreased volume of the amygdala-uncus, bilateral insular cortices, ACC, temporal cortex and the left thalamus in schizophrenics was noted.

In the limbic and paralimbic systems, patients with schizophrenia showed reduction of volumes in the parahippocampal gyri, amygdala-uncus, insular cortices and the anterior cingulate cortices (ACC). They also demonstrated reduced volumes in the frontal and temporal association areas, dorsal premotor areas and the left thalamus. In comparison with controls, patients with schizophrenia showed significantly increased volume in the CSF space such as lateral ventricle, sylvian and the interhemispheric fissures but not in the grey matter (Table 2 and Fig. 4).

Morphological changes associated with the Val158Met polymorphism (genotype effects)

In comparison with Met-COMT carriers, individuals homozygous for the Val-COMT allele demonstrated a significant reduction of volumes in the left ACC and the right middle temporal gyrus (MTG) (Table 2 and Fig. 5). The hypothesis-driven analysis demonstrated a genotype effect on volumes in the bilateral DLPFC (right BA9, left BA8) at a lenient threshold (uncorrected $P = 0.05$) (data are not shown), however, no voxels could survive after the correction for multiple comparisons (FDR < 0.05) within the ROI. There were no areas that individuals homozygous for the Val-COMT allele demonstrated a significant increment of volume compared to Met-COMT carriers.

Genotype—diagnosis interaction effects

We found significant genotype-diagnosis interaction effects on brain morphology. The stronger effects of Val158Met polymorphism on brain morphology in schizophrenia than those in controls were noted in the left ACC and the left amygdala-uncus (Table 2 and Fig. 6). The hypothesis-driven analysis demonstrated a genotype-diagnosis interaction effect on the volume of the right DLPFC (BA9/46) at a lenient threshold (uncorrected $P = 0.05$) (data not shown), however, no voxels could survive after the correction of multiple comparisons (FDR < 0.05) within the ROI.

Effects of the Val58Met polymorphism on brain morphology

Since genotype–disease interaction effects were found, we estimated the effects of genotypes on brain morphology in the control groups and the schizophrenic groups separately.

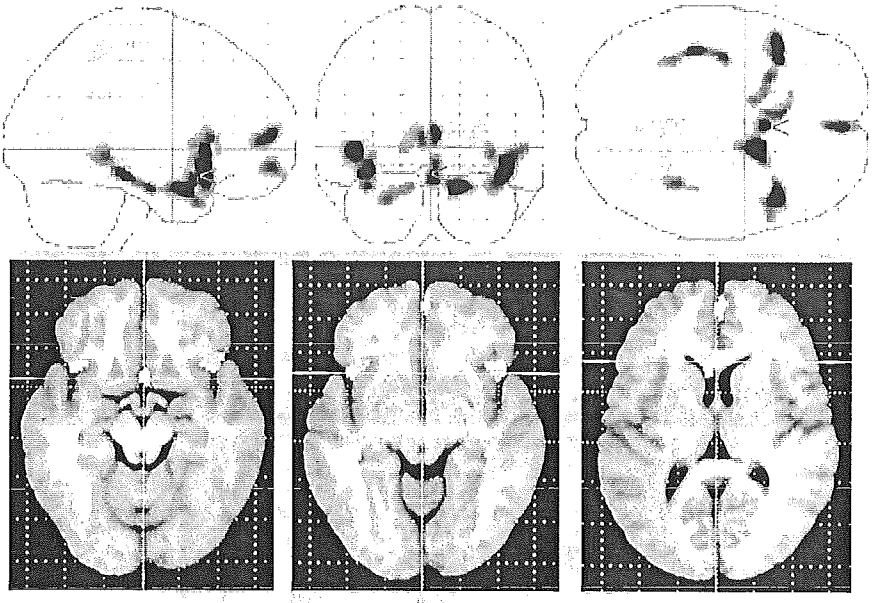

Fig. 4 Increased volumes in schizophrenics as compared to controls. *Top*: The SPM {*t*} is displayed in a standard format as a MIP. Patients with schizophrenia showed a significantly increased volume of the CSF space. *Bottom*: The SPM {*t*} is displayed onto axial T_1-weighted MR images. A significantly increased volume of the CSF space such as the lateral ventricle, sylvian fissures and the interhemisphrenic fissure was noted.

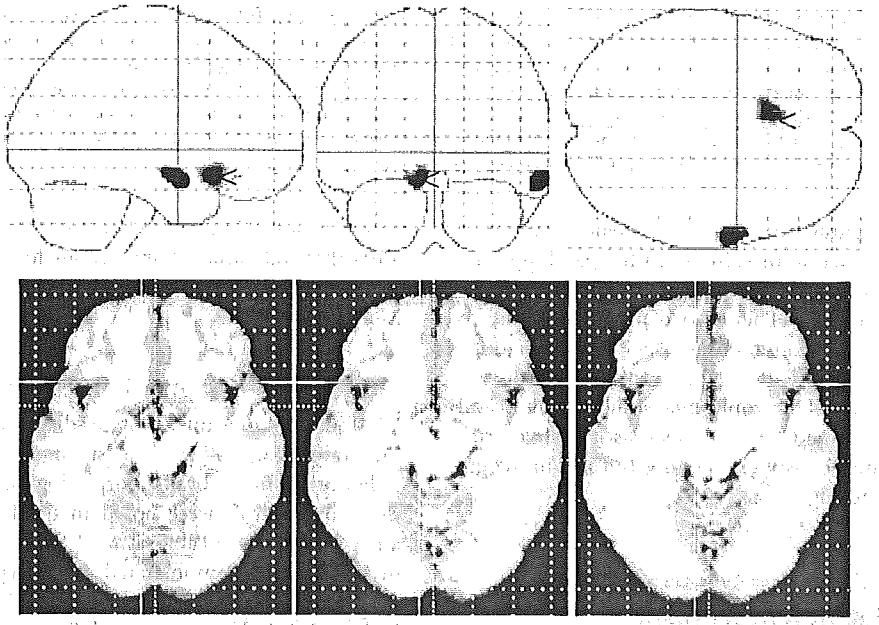

Fig. 5 The result of comparison between individuals homozygous for the Val-COMT allele (n = 57) and Met-COMT carriers (n = 66) (genotype effects). *Top*: Representation in stereotaxic space of regions with significant reduction of volume in individuals homozygous for the Val-COMT allele demonstrated. *Bottom*: The SPM {*t*} is displayed onto axial T_1-weighted MR images. Individuals homozygous for the Val-COMT allele demonstrated a significant reduction of volumes in the left ACC and right MTG as compared to Met-COMT carriers.

In the control group, we found no significant morphological differences between individuals homozygous for the Val-COMT allele and Met-COMT carriers. Even the hypothesis driven analysis with a lenient statistical threshold ($P < 0.05$) could not detect any significant morphological changes in the DLPFC between the two groups. Contrary to the control group, schizophrenics homozygous for the Val-COMT allele showed a significant reduction of volumes in the left amygdala-uncus, bilateral ACC, right MTG and the left thalamus when compared to the patients carrying the Met-COMT

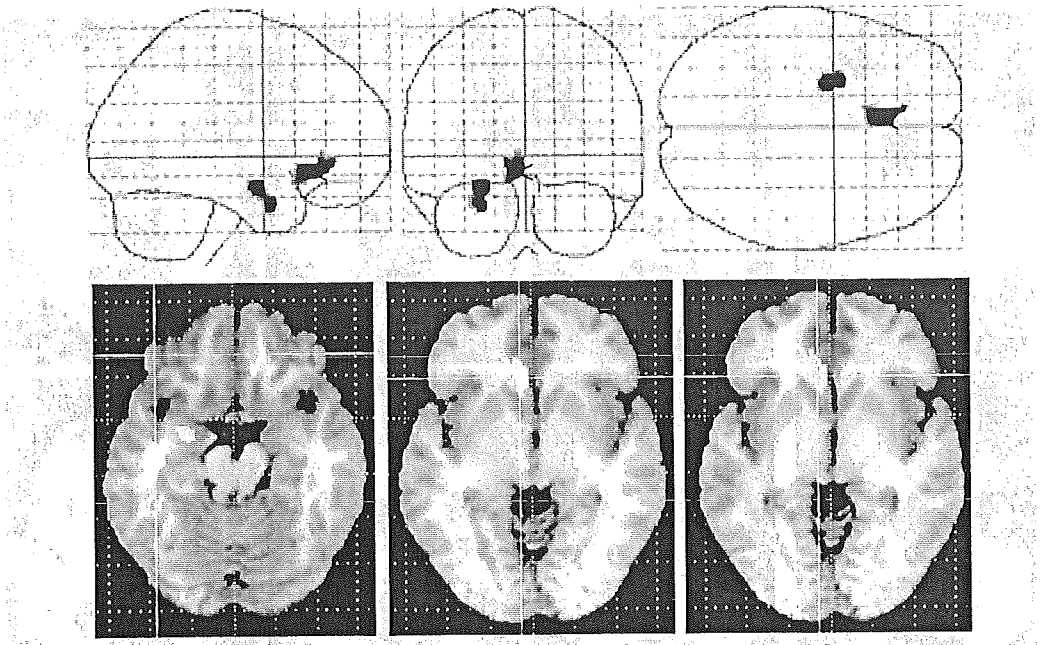

Fig. 6 Results of genotype-diagnosis interaction effects on brain morphology. *Top*: The SPM {*t*} is displayed in a standard format as a MIP. The stronger effects of Val158Met polymorphism on brain morphology in schizophrenia than those in controls were noted in the left ACC, left parahippocampal gyrus and the amygdala-uncus. *Bottom*: The SPM {*t*} is displayed onto axial T_1-weighted MR images.

allele (Table 2, Fig. 7). The hypothesis-driven analysis demonstrated a significantly decreased volume of the bilateral DLPFC in schizophrenics homozygous for the Val-COMT allele when compared to the Met-COMT schizophrenics at a lenient threshold (uncorrected $P = 0.05$) (data not shown). However, no voxels could survive after the correction for multiple comparisons (FDR < 0.05) within the ROI. There are no significantly increased volumes in the schizophrenics homozygous for the Val-COMT allele. All the results were essentially unchanged even if all the left-handed subjects were excluded in all analyses (data not shown).

Discussion

In this study, we found reduction of volumes in the limbic and paralimbic systems, neocortical areas (prefrontal and temporal cortices) and thalamus in patients with schizophrenia when compared to control subjects. The schizophrenia patients demonstrated a significant enlargement of CSF spaces including the lateral and sylvian fissure, which could be interpreted as a result of impaired neurodevelopment and/or global brain atrophy. These findings are concordant with previous studies of MR morphometry of schizophrenia. According to a recent review and meta-analyses of the morphometry of schizophrenia, the consistent abnormalities in schizophrenia are as follows; (i) ventricular enlargement (lateral and third ventricles); (ii) medial temporal lobe involvement; (iii) superior temporal gyrus involvement (iv) parietal lobe involvement; and (v) subcortical brain region involvement including the thalamus (Okubo *et al.*, 2001; Shenton *et al.*, 2001; Davidson and Heinrichs, 2003). The other regions observed in this study, such as the insula, DLPFC and the ACC have also often been demonstrated as abnormal areas in schizophrenia (Shenton *et al.*, 2001; Takahashi *et al.*, 2004; Yamasue *et al.*, 2004). Using the TBM technique, we replicated the morphological abnormalities observed in previous MR studies on schizophrenia, suggesting that TBM was able to detect morphological changes associated with this disease. As well as neuroimaging studies, post-mortem studies have also reported morphological abnormalities in schizophrenia, but not necessarily as common neuropathological features. Regions including the hippocampus, ACC, thalamus and the DLPFC are regularly associated with abnormalities of cell size, cell number and neuronal organization (Bogerts, 1993; Arnold and Trojanowski, 1996; Selemon, 2001; Selemon and Lynn, 2002, 2003). Selemon *et al.* reported that schizophrenics demonstrated abnormalities in overall and laminar neuronal density in the DLPFC (Brodmann area 9) and suggested that the DLPFC should be a particularly vulnerable target in the disease process (Selemon 2001; Selemon and Lynn, 2002, 2003).

Importantly, our results suggest that some of the morphological changes in schizophrenia mentioned above are associated with the Val158Met polymorphism of the COMT gene. In the schizophrenic group, the polymorphism was associated with the volumes in the limbic and paralimbic systems, temporal cortices and the left thalamus, whereas no morphological changes related to the polymorphism were found in

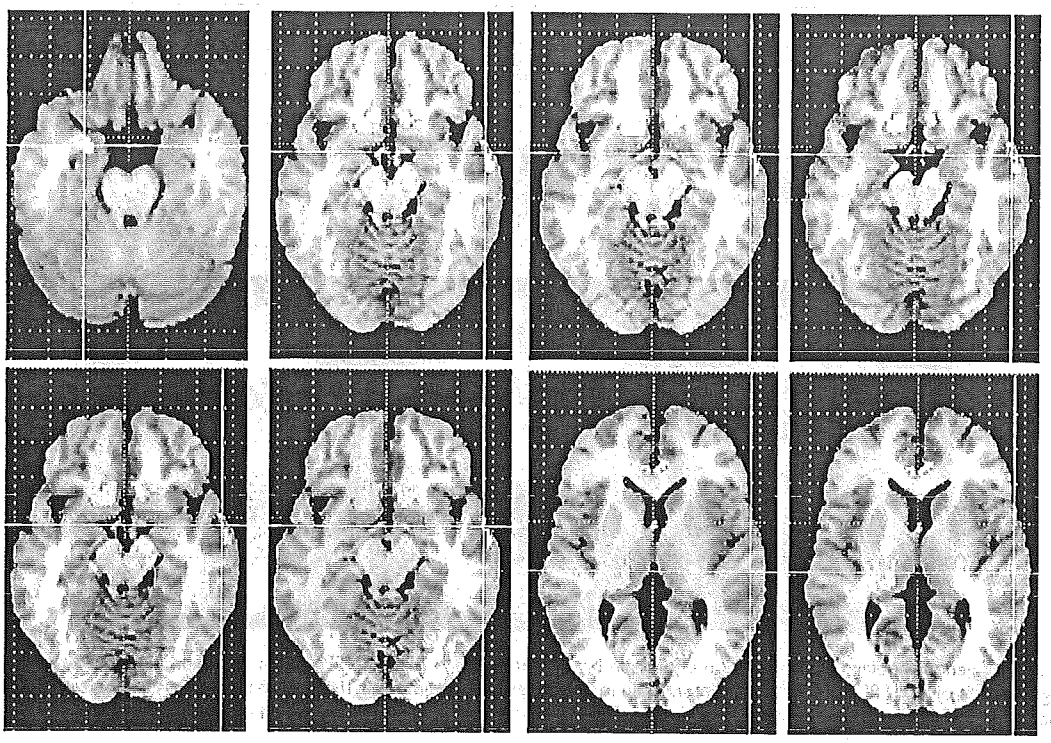

Fig. 7 The effects of the Val158Met polymorphism of the COMT gene on brain morphology in schizophrenics. The SPM {*t*} is displayed onto axial T_1-weighted MR images. The schizophrenics homozygous for the Val-COMT allele ($n = 19$) showed a significant reduction of volumes in the left parahippocampal gyrus, amygdala-uncus, ACC, left thalamus and the right MTG when compared to patients who carried the Met-COMT allele ($n = 28$).

normal individuals. As a consequence, significant genotype-diagnosis interaction effects were found in the left ACC and the amygdala-uncus. These results indicate that the Val158-Met polymorphism of the COMT gene is strongly associated with morphological changes in schizophrenia, particularly those in the limbic and paralimbic systems. Longitudinal MRI studies of schizophrenia strongly suggest that progressive changes should occur after onset of the illness (Okubo *et al.*, 2001; Ho *et al.*, 2003). Recent studies have demonstrated that antipsychotic drugs, particularly haloperidol, have considerable effects on brain morphology (Arango *et al.*, 2003; Lieberman, 2005; Dorph *et al.*, 2005). Because of the long duration of illness and medication taken by our subjects, the effects of antipsychotics may be a possible confounding factor for our findings. However, the duration of medication and the dose of antipsychotics taken by the Val/Val-COMT schizophrenics did not differ from those of the Met-COMT schizophrenics. Although the effects of antipsychotics on brain morphology may contribute to the observed morphological changes in patients with schizophrenia in this study, it is unlikely that the effects of antipsychotics contributed to morphological differences between the two schizophrenic groups.

When we were preparing this manuscript, another study demonstrated no genotype and genotype-diagnosis interaction effects of the Val158Met polymorphism on morphology of the frontal lobe in controls and schizophrenia (Ho *et al.*, 2005). Although there are differences between the two studies, such as mean ages of subjects, duration of illness, methods for image analysis and a racial factor (Caucasians versus Japanese), that study also demonstrated no genotype and genotype-diagnosis interaction effects on morphology of the DLPFC. However, we found these effects on DLPFC morphology at a very lenient statistical threshold. Further studies with a larger sample will clarify whether Val158Met polymorphism does affect DLPFC morphology. As well as prefrontal morphology, we found no significant genotype or genotype-diagnosis interaction effects on working memory, however, schizophrenics homozygous for the Val-COMT allele tended to have poorer performances on working memory measures, compared to Met-COMT carriers with schizophrenia. Although there were no significant effects of Val158Met polymorphism on working memory and other neuropsychological measures, a significant effect of the polymorphism was noted in brain morphology. The brain morphology has been considered to be useful as an intermediate phenotype in genetic research in neuropsychiatric disorders (Baare *et al.*, 2001; Durston *et al.*, 2005). Therefore, morphological changes might be more sensitive to the effects of genotype than behavioural measures such as the performance of working memory measures. In a previous study (Ho *et al.*, 2005) a similar phenomenon—no significant effect of Val158Met polymorphism on working memory performance but significant

effects on brain activities during a working memory task—was found. Further studies with a larger sample size are needed to clarify whether morphological changes are a more sensitive marker of genotype effects than behavioural measures.

Unexpectedly, we found effects of the polymorphism on the ACC volume rather than the DLPFC which is crucial for working memory. Since the ACC is associated with a variety of cognitive tasks involving mental efforts, and also plays important roles in working memory (Paus *et al.*, 2001; Kondo *et al.*, 2004), it is feasible that the Val158Met polymorphism may be associated with the ACC morphology. In fact, a previous study demonstrated that the Val-COMT allele was associated with abnormal ACC function as well as abnormal prefrontal cortical function, relative to the Met-COMT allele, as measured by cognitive tests and fMRI activation in normal subjects (Egan *et al.*, 2001).

One would argue that the effects of one polymorphism of the gene could not explain the morphological changes in schizophrenia. As well as the effects of the Val158Met polymorphism, we agree that other polymorphisms of schizophrenia susceptibility genes and genotype–genotype interaction may relate to individual brain morphology. Such interactions might contribute to the different effects of the Val158Met polymorphism on brain morphology observed in this study. Further studies of each effect and interaction of several schizophrenia susceptibility genes on brain morphology, brain functions and performances of neuropsychological tests should be conducted to clarify how polymorphisms of these genes affect intermediate phenotypes of schizophrenia.

In conclusion, we found an association between the Val158Met polymorphism and morphological abnormalities in schizophrenia. Although the underlying mechanisms of our observation remain to be clarified, our data indicate that brain morphology as an intermediate phenotype should be useful for investigating how genotypes affect endophenotypes of schizophrenia.

Acknowledgements

This study was supported by the Promotion of Fundamental Studies in Health Science of Organization for Pharmaceuticals and Medical Devices Agency. This work was also supported in part by Grants-in-Aid from the Japanese Ministry of Health, Labor and Welfare (H17-kokoro-007 and H16-kokoro-002), the Japanese Ministry of Education, Culture, Sports, Science and Technology and Core research for Evolutional Science and Technology of Japan Science and Technology Agency, Japan Foundation for Neuroscience and Mental Health.

References

Arango C, Breier A, McMahon R, Carpenter WT Jr, Buchanan RW. The relationship of clozapine and haloperidol treatment response to prefrontal, hippocampal, and caudate brain volumes. Am J Psychiatry 2003; 160: 1421–7.

Arnold SE, Trojanowski JQ. Recent advances in defining the neuropathology of schizophrenia. Acta Neuropathol (Berl) 1996; 92: 217–31.

Ashburner J, Friston KJ. High-dimensional image warping. In: Frackowiak R, editor. Human brain function. 2nd edn. Academic Press; 2004. p. 673–94.

Baare WF, Hulshoff Pol HE, Boomsma DI, Posthuma D, de Geus EJ, Schnack HG, et al. Quantitative genetic modeling of variation in human brain morphology. Cereb Cortex 2001; 11: 816–24.

Bogerts B. Recent advances in the neuropathology of schizophrenia. Schizophr Bull 1993; 19: 431–45.

Cannon TD, Mednick SA, Parnas J, Schulsinger F, Praestholm J, Vestergaard A. Developmental brain abnormalities in the offspring of schizophrenic mothers. I. Contributions of genetic and perinatal factors. Arch Gen Psychiatry 1993; 50: 551–64.

Chen J, Lipska BK, Halim N, Ma QD, Matsumoto M, Melhem S, et al. Functional analysis of genetic variation in catechol-O-methyltransferase (COMT): effects on mRNA, protein, and enzyme activity in postmortem human brain. Am J Hum Genet 2004; 75: 807–21.

Daniels JK, Williams NM, Williams J, Jones LA, Cardno AG, Murphy KC, et al. No evidence for allelic association between schizophrenia and a polymorphism determining high or low catechol O-methyltransferase activity. Am J Psychiatry 1996; 153: 268–70.

Davidson LL, Heinrichs RW. Quantification of frontal and temporal lobe brain-imaging findings in schizophrenia: a meta-analysis. Psychiatry Res 2003; 122: 69–87.

Dorph Petersen KA, Pierri JN, Perel JM, Sun Z, Sampson AR, Lewis DA. The influence of chronic exposure to antipsychotic medications on brain size before and after tissue fixation: a comparison of haloperidol and olanzapine in macaque monkeys. Neuropsychopharmacology 2005; 30: 1649–61.

Durston S, Fossella JA, Casey BJ, Hulshoff Pol HE, Galvan A, Schnack HG, et al. Differential effects of DRD4 and DAT1 genotype on fronto-striatal gray matter volumes in a sample of subjects with attention deficit hyperactivity disorder, their unaffected siblings, and controls. Mol Psychiatry 2005; 10: 678–85.

Egan MF, Goldberg TE, Kolachana BS, Callicott JH, Mazzanti CM, Straub RE, et al. Effect of COMT Val108/158 Met genotype on frontal lobe function and risk for schizophrenia. Proc Natl Acad Sci USA 2001; 98: 6917–22.

Fan JB, Zhang CS, Gu NF, Li XW, Sun WW, Wang HY, et al. Catechol-O-methyltransferase gene Val/Met functional polymorphism and risk of schizophrenia: a large-scale association study plus meta-analysis. Biol Psychiatry 2005; 57: 139–44.

Galderisi S, Maj M, Kirkpatrick B, Piccardi P, Mucci A, Invernizzi G, et al. COMT Val(158)Met and BDNF C(270) T polymorphisms in schizophrenia: a case-control study. Schizophr Res 2005; 73: 27–30.

Gaser C, Nenadic I, Buchsbaum BR, Hazlett EA, Buchsbaum MS. Deformation-based morphometry and its relation to conventional volumetry of brain lateral ventricles in MRI. Neuroimage 2001; 13: 1140–5.

Gogtay N, Sporn A, Clasen LS, Greenstein D, Giedd JN, Lenane M, et al. Structural brain MRI abnormalities in healthy siblings of patients with childhood-onset schizophrenia. Am J Psychiatry 2003; 160: 569–571.

Goldberg TE, Egan MF, Gscheidle T, Coppola R, Weickert T, Kolachana BS, et al. Executive subprocesses in working memory: relationship to catechol-O-methyltransferase Val158Met genotype and schizophrenia. Arch Gen Psychiatry 2003; 60: 889–96.

Gurtin, ME. An introduction to continuum mechanics. Boston: Academic Press; 1987.

Harrison PJ, Weinberger DR. Schizophrenia genes, gene expression, and neuropathology: on the matter of their convergence. Mol Psychiatry 2005; 10: 40–68.

Hashimoto R, Yoshida M, Ozaki N, Yamanouchi Y, Iwata N, Suzuki T, et al. Association analysis of the -308G>A promoter polymorphism of the tumor necrosis factor alpha (TNF-alpha) gene in Japanese patients with schizophrenia. J Neural Transm 2004; 111: 217–21.

Hashimoto R, Yoshida M, Kunugi H, Ozaki N, Yamanouchi Y, Iwata N, et al. A missense polymorphism (H204R) of a Rho GTPase-activating protein, the chimerin 2 gene, is associated with schizophrenia in men. Schizophr Res 2005; 73: 383–5.

Ho BC, Andreasen NC, Nopoulos P, Arndt S, Magnotta V, Flaum M. Progressive structural brain abnormalities and their relationship to clinical outcome: a longitudinal magnetic resonance imaging study early in schizophrenia. Arch Gen Psychiatry 2003; 60: 585–94.

Ho BC, Wassink TH, O'leary DS, Sheffield VC, Andreasen NC. Catechol-O-methyl transferase Val(158)Met gene polymorphism in schizophrenia: working memory, frontal lobe MRI morphology and frontal cerebral blood flow. Mol Psychiatry 2005; 10: 287–98.

Kendler KS. Overview: a current perspective on twin studies of schizophrenia. Am J Psychiatry 1983; 140: 1413–25.

Kondo H, Osaka N, Osaka M. Cooperation of the anterior cingulate cortex and dorsolateral prefrontal cortex for attention shifting. Neuroimage 2004; 23: 670–9.

Kunugi H, Vallada HP, Sham PC, Hoda F, Arranz MJ, Li T, et al. Catechol-O-methyltransferase polymorphisms and schizophrenia: a transmission disequilibrium study in multiply affected families. Psychiatr Genet 1997; 7: 97–101.

Lieberman JA, Tollefson GD, Charles C, Zipursky R, Sharma T, Kahn RS, et al. Antipsychotic drug effects on brain morphology in first-episode psychosis. Arch Gen Psychiatry 2005; 62: 361–70.

Maldjian JA, Laurienti PJ, Kraft RA, Burdette JH. An automated method for neuroanatomic and cytoarchitectonic atlas-based interrogation of fMRI data sets. Neuroimage 2003; 19: 1233–9.

McGue M, Gottesman II, Rao DC. The transmission of schizophrenia under a multifactorial threshold model. Am J Hum Genet 1983; 35: 1161–78.

Nelson KB, Lynch JK. Stroke in newborn infants. Lancet Neurol 2004; 3: 150–8.

Norton N, Kirov G, Zammit S, Jones G, Jones S, Owen R, et al. Schizophrenia and functional polymorphisms in the MAOA and COMT genes: no evidence for association or epistasis. Am J Med Genet 2002; 114: 491–6.

Ohmori O, Shinkai T, Kojima H, Terao T, Suzuki T, Mita T, et al. Association study of a functional catechol-O-methyltransferase gene polymorphism in Japanese schizophrenics. Neurosci Lett 1998; 243: 109–12.

Okubo Y, Saijo T, Oda K. A review of MRI studies of progressive brain changes in schizophrenia. J Med Dent Sci 2001; 48: 61–7.

Palmatier MA, Kang AM, Kidd KK. Global variation in the frequencies of functionally different catechol-O-methyltransferase alleles. Biol Psychiatry 1999; 46: 557–67.

Paus T. Primate anterior cingulate cortex: where motor control, drive and cognition interface. Nat Rev Neurosci 2001; 2: 417–24.

Pezawas L, Verchinski BA, Mattay VS, Callicott JH, Kolachana BS, Straub RE, et al. The brain-derived neurotrophic factor val66met polymorphism and variation in human cortical morphology. J Neurosci 2004; 24: 10099–102.

Selemon LD. Regionally diverse cortical pathology in schizophrenia: clues to the etiology of the disease. Schizophr Bull 2001; 27: 349–77.

Shenton ME, Dickey CC, Frumin M, McCarley RW. A review of MRI findings in schizophrenia. Schizophr Res 2001; 49: 1–52.

Steel RM, Whalley HC, Miller P, Best JJ, Johnstone EC, Lawrie SM. Structural MRI of the brain in presumed carriers of genes for schizophrenia, their affected and unaffected siblings. J Neurol Neurosurg Psychiatry 2002; 72: 455–8.

Stefanis NC, Van Os J, Avramopoulos D, Smyrnis N, Evdokimidis I, Hantoumi I, et al. Variation in catechol-O-methyltransferase val158 met genotype associated with schizotypy but not cognition: a population study in 543 young men. Biol Psychiatry 2004; 56: 510–5.

Sullivan PF, Kendler KS, Neale MC. Schizophrenia as a complex trait: evidence from a meta-analysis of twin studies. Arch Gen Psychiatry 2003; 60: 1187–92.

Takahashi T, Suzuki M, Hagino H, Zhou SY, Kawasaki Y, Nohara S, et al. Bilateral volume reduction of the insular cortex in patients with schizophrenia: a volumetric MRI study. Psychiatry Res 2004; 132: 187–96.

Talairach J, Tournoux P. A coplanar stereotaxic atlas of a human brain. Three-dimensional proportional system: an approach to cerebral imaging. Stuttgart: Thieme; 1988.

Tunbridge EM, Bannerman DM, Sharp T, Harrison PJ. Catechol-O-methyltransferase inhibition improves set-shifting performance and elevates stimulated dopamine release in the rat prefrontal cortex. J Neurosci 2004; 24: 5331–5.

Weinberger DR, Egan MF, Bertolino A, Callicott JH, Mattay VS, Lipska BK, et al. Prefrontal neurons and the genetics of schizophrenia. Biol Psychiatry 2001; 50: 825–44.

Wright IC, McGuire PK, Poline JB, Travere JM, Murray RM, Frith CD, et al. A voxel-based method for the statistical analysis of gray and white matter density applied to schizophrenia. Neuroimage 1995; 2: 244–52.

Yamasue H, Iwanami A, Hirayasu Y, Yamada H, Abe O, Kuroki N, et al. Localized volume reduction in prefrontal, temporolimbic, and paralimbic regions in schizophrenia: an MRI parcellation study. Psychiatry Res 2004; 131: 195–207.

Available online at www.sciencedirect.com
SCIENCE DIRECT®
Neuroscience Letters 397 (2006) 25–29
Neuroscience Letters
www.elsevier.com/locate/neulet

The Val66Met polymorphism of the brain-derived neurotrophic factor gene affects age-related brain morphology

Kiyotaka Nemoto [a,e], Takashi Ohnishi [a,b,c,*], Takeyuki Mori [a,c], Yoshiya Moriguchi [a], Ryota Hashimoto [c], Takashi Asada [d], Hiroshi Kunugi [c]

[a] *Department of Radiology, National Center Hospital for Mental, Nervous and Muscular Disorders, National Center of Neurology and Psychiatry, 4-1-1, Ogawahigashi, Kodaira, Tokyo 187-8551, Japan*
[b] *Department of Investigative Radiology, Research Institute, National Cardiovascular Center, 5-7-1 Fujishirodai, Suita, Osaka 565-8565, Japan*
[c] *Department of Mental Disorder Research, National Institute of Neuroscience, National Center of Neurology and Psychiatry, 4-1-1 Ogawahigashi, Kodaira, Tokyo 187-8551, Japan*
[d] *Department of Neuropsychiatry, Institute of Clinical Medicine, University of Tsukuba, 1-1-1 Tennoudai, Tsukuba, Ibaraki 305-8575, Japan*
[e] *Department of Psychiatry, Ibaraki Prefectural Tomobe Hospital, 654 Asahicho, Tomobe, Ibaraki 309-1717, Japan*

Received 18 October 2005; received in revised form 22 November 2005; accepted 30 November 2005

Abstract

We investigated the effects of the brain-derived neurotrophic factor (BDNF) Val66Met polymorphism on age-associated changes of brain morphology in 109 Japanese healthy subjects using MRI with optimized voxel-based morphometry technique. A significant age-related volume reduction was found in the dorsolateral prefrontal cortices (DLPFC), anterior cingulate cortices, and temporal and parietal cortices in all subjects. Further analysis revealed a significantly negative correlation between age and the volume of the bilateral DLPFC only in the Met-BDNF carriers, and a significant interaction between the polymorphism and age-associated volume changes in the bilateral DLPFC. Furthermore, Met-carriers showed a significant interaction ($p < 0.0001$) between the gender and the genotype on the gray matter volume in the DLPFC, and female Met-carriers showed more widespread age-associated volume reduction in DLPFC than male Met-carriers. Our data suggest that the Val66Met polymorphism may impact on age-related changes of the brain, which might be associated with the functional variance of neuroprotective effects of the BDNF. Furthermore, we suggest that genotype effects of the BDNF gene on brain morphology might differ in female from in male.

Keywords: Brain-derived neurotrophic factor; Val66Met polymorphism; Magnetic resonance imaging; Voxel-based morphometry; Dorsolateral prefrontal cortex; Aging

Brain-derived neurotrophic factor (BDNF), a member of neurotrophin family, has important roles in hippocampal plasticity and hippocampal-related learning and memory through long-term potentiation [15]. It also plays an important role in preventing death of neurons during development and protecting cholinergic neurons of the basal forebrain and the hippocampus from induced death in the adult brain [21].

A common missense polymorphism of the BDNF gene producing a valine to methionine amino acid substitution (Val66Met) affects the activity dependent secretion of BDNF in neurons and affects memory function [6,8]. Neuroimaging studies revealed that this polymorphism affected memory-related neuronal activities measured by functional magnetic resonance imaging (MRI) and macroscopic morphology of the hippocampus [8,12,23,28]. Regarding the brain morphology in normal individuals, Pezawas et al. [23] reported that Met-BDNF carriers had smaller volumes of the hippocampi and the prefrontal cortices as compared to individuals with homozygous Val-BDNF. This result was recently replicated in another mixed study of healthy and schizophrenic subjects [28]. Although several neuroimaging studies have indicated that environmental factors considerably impact on human brain structures even in normal adult brains [18], these data suggest that genetic factors such as polymorphism of BDNF might also strongly affect human brain morphology, and contribute to individual differences of brain morphology.

Aging is another factor which strongly affects brain morphology in human. There are several studies that demon-

* Corresponding author. Tel.: +81 42 341 2711; fax: +81 42 346 1790.
E-mail address: tohnishi@hotmail.com (T. Ohnishi).

0304-3940/$ – see front matter © 2005 Elsevier Ireland Ltd. All rights reserved.
doi:10.1016/j.neulet.2005.11.067

strated morphological changes associated with normal aging in vivo [10,24]. A general trend in the in vivo volumetric studies of healthy volunteers points to the prefrontal cortex as the cortical region in which the largest age-related volume reduction is observed. Considering the previous findings that BDNF is expressed abundantly in the prefrontal cortex [25] and that BDNF has a neuroprotective effect, Val66Met polymorphism might have some impacts on age-related morphological changes. However, there is no datum whether this polymorphism is associated with age-related morphological changes.

To clarify whether the BDNF polymorphism impacts on morphological changes associated with aging, we analyzed structural MR images in 109 normal individuals using optimized voxel-based morphometry (VBM) technique.

One hundred and thirty healthy subjects participated in the study. Written informed consent was obtained from all subjects in accord with ethical guidelines in place at local ethical committee. All of the subjects were recruited from local advertisements and underwent a Japanese version of National Adult Reading Test (JART) that is essentially the same as National Adult Reading Test [22] and MRI scanning. We employed JART as a convenient tool to measure IQ for each participant because previous study reported that it showed high correlation with IQ in healthy subjects [20]. All subjects were screened by a questionnaire regarding medical history and excluded if they had neurological, psychiatric or medical conditions that could potentially affect the central nervous system, such as substance abuse or dependence, atypical headache, head trauma with loss of consciousness, asymptomatic or symptomatic cerebral infarction detected by T2 weighted MRI, hypertension, chronic lung disease, kidney disease, chronic hepatic disease, cancer, or diabetes mellitus. Template creation for the optimized VBM was based on a sample of the 120 subjects, aged 36.2 ± 12.1 years (range 20–72). All subjects were Japanese. Since single nucleotide polymorphism (SNP) genotyping, described in the next section, was done successfully in 109 subjects, the MR images of these 109 subjects were used for subsequent analyses. According to the polymorphism, subjects were categorized into the following three groups: a homozygous Val-BDNF group ($n=41$), a Val/Met-BDNF group ($n=51$), or a homozygous Met-BDNF group ($n=17$). The genotype distribution of this SNP was not deviated with Hardy–Weinberg equilibrium (chi-square = 0.03, $p=0.86$). Because of the small number of subjects with homozygous Met-BDNF, the Val/Met-BDNF group and homozygous Met-BDNF group were treated as one group, the Met-BDNF carriers ($n=68$). The demographic data of these groups are the following; the homozygous Val-BDNF comprised 26 females and 15 males, two were left-handed, aged 36.9 ± 13.0 years (range 21–68), and the mean education period and JART score were 16.2 ± 2.8 years (range 12–24) and 75.5 ± 13.3 (equivalent to 108.8 ± 9.55 for full scale IQ (range 50–96; equivalent to 90.5–123.6 for full scale IQ), respectively. The Met-BDNF carriers comprised 45 females and 23 males, three were left-handed, aged 35.8 ± 11.6 years (range 20–72), and their mean education period and JART score were 16.9 ± 3.0 years (range 12–28) and 78.0 ± 11.6 (equivalent to 110.7 ± 8.3) for full scale IQ (range 45–99; equivalent to 86.9–125.8 for full scale IQ), respectively. The mean age, gender ratio, handedness, education period, or JART score did not differ between the two groups (two sample t-test, data not shown).

The detail process of genotyping of BDNF Val66Met SNP (dbSNP accession: rs6265) was described previously [13]. Primers and probes for detection of the SNP (TaqMan SNP Genotyping assays on demand) were purchased from Applied Biosystems (ABI, Foster City, CA, USA). PCR cycling conditions were: at 95 °C for 10 min, 50 cycles of 92 °C for 15 s and 60 °C for 1 min.

All MR studies were performed on a 1.5 T Siemens Magnetom Vision plus system. A three dimensional volumetric acquisition of a T1-weighted gradient echo sequence produced a gapless series of 144 sagittal sections using an MPRage sequence (TE/TR, 4.4/11.4 ms; flip angle, 15°; acquisition matrix, 256 × 256; 1NEX, field of view, 31.5 cm; slice thickness, 1.23 mm).

Data were analyzed with Statistical Parametric Mapping 2 (SPM2) (http://www.fil.ion.ucl.ac.uk/spm/; Wellcome Department of Imaging Neuroscience, London, UK) running on MATLAB 6.5 R1 (MathWorks, Natick, MA). Before analyses, each image was confirmed by a neuroradiologist to eliminate images with artifacts, and then anterior commissure–posterior commissure line was adjusted. First, we made a customized anatomical T1 template and prior probability images from the sample of 120 brains [10]. Then, images were processed using an optimized VBM script (dbm.neuro.uni-jena.de/vbm.html). The detail of this process is described elsewhere [2,10]. The normalized segmented images were modulated by multiplication with Jacobian determinants of the spatial normalization function to encode the deformation field for each subject as tissue density changes in the normal space. Finally, images were smoothed using a 12 mm full width half maximum of isotropic Gaussian kernel. Statistical analyses were performed with SPM2, which implemented a General Linear Model. Proportional scaling was used to achieve global normalization of voxel values between images. First, we used a two-sample t-test to test regional population effect on gray matter volume. For this analysis, we set $p<0.005$ without a correction for multiple comparisons, followed by applying small volume correction to each cluster with a false discovery rate (FDR) < 0.05. For the small volume correction, spheres with radius 10 mm around the peak were set as regions of interest (ROIs). The resulting sets of t-values constituted the statistical parametric maps {SPM (t)}. Anatomic localization was according to both MNI coordinates and Talairach coordinates, obtained from M. Brett's transformations (http://www.mrc-cbu.cam.ac.uk/Imaging/Common/mnispace.shtml) and presented as Talairach coordinates. Since a previous study with Caucasians demonstrated a significant reduction of volumes in the hippocampi and the frontal cortices in Met-BDNF carriers, we applied an additional hypothesis-driven ROI method to test regional population effects in these regions by using the Wake Forest University PickAtlas [19].

The genotype effects on age-related morphological changes were tested using a single subject condition and covariate model. Since several studies reported gender different age-related mor-

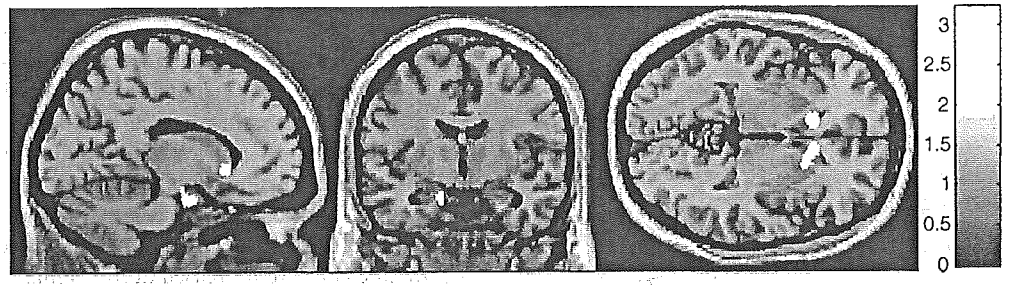

Fig. 1. The volume reduction of Met-BDNF carriers compared to that of individuals with homozygous Val-BDNF ($p < 0.05$, small volume correction with FDR). A significant reduction of volumes of the left parahippocampal gyrus (t-value: 2.92, Talairach coordinates (TAL): −12, −3, −19) and the bilateral heads of caudate nucleus (left: t-value; 3.23, TAL: −9, 22, −3, right: t-value; 3.02, TAL: 10, 21, −4) in the Met-BDNF carriers was noted.

phological changes in the brain [7], we additionally examined genotype effects on age-related morphological changes in each gender, separately. Orthogonalized first order polynomial expansion of age was treated as a covariate of interest to determine the linear effects of age [5]. Since second- and third-order polynomial expansions did not contribute to the age effect model of our sample, we removed them from a design matrix. Considering the possible association between IQ and brain morphology, we treated JART score as a nuisance variable. For this analysis, we applied $p < 0.001$, corrected for multiple comparisons with FDR < 0.05 as a statistical threshold [9]. MarsBar program (marsbar.sourceforge.net/) was also used to extract data from the regions of interest.

Fig. 1 shows a significant reduction of gray matter volumes of the left parahippocampal gyrus (Brodmann area (BA) 34), and bilateral heads of the caudate nucleus in Met-BDNF carriers when compared to homozygous Val-BDNF individuals. Even in hypothesis-driven ROI approach with a lenient statistical threshold (uncorrected $p = 0.05$), we could not find any significant differences of hippocampal nor prefrontal cortical volumes between the two groups. The results were essentially unchanged even when the restricted samples of subjects (female group, male group, or young group aged under 40 years old) were analyzed (data not shown).

Fig. 2 shows morphological changes related to normal aging. A significant negative correlation between age and the gray matter volumes was noted in the bilateral dorsolateral prefrontal cortices (DLPFC; BA9, 46), right superior temporal gyrus (STG; BA22), bilateral insulae (BA13), bilateral caudate nuclei, left anterior cingulate gyrus (BA24), bilateral inferior parietal lobules (BA40), bilateral precunei (BA7), and bilateral fusiform gyri (BA37) in all subjects. In homozygous Val-BDNF individuals, a significant age-related volume reduction was found in the bilateral insulae (BA13) and right STG (BA22). On the other hand, Met-BDNF carrier showed an additional negative correlation of the gray matter volumes in the bilateral DLPFC (BA9, 46) and right dorsal premotor area (BA6) with age. Additional analyses in each gender revealed a significant interaction ($p < 0.0001$) in Met-carriers between the gender and the genotype on the gray matter volume in the DLPFC, and female Met-carriers showed more widespread age-associated volume reduction in DLPFC than male Met-carriers. Male Met-carrier also showed volume

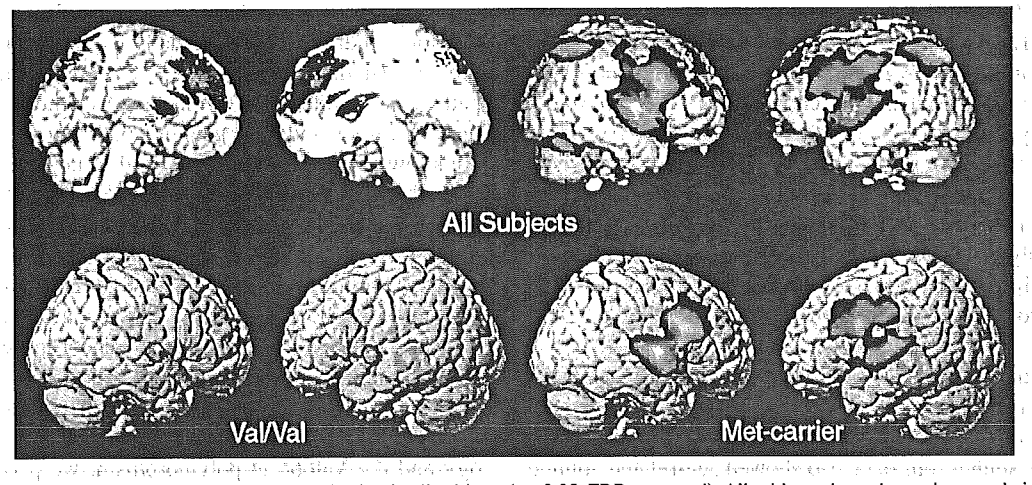

Fig. 2. (Top) The volume reduction associated with normal aging in all subjects ($p < 0.05$, FDR corrected). All subjects showed negative correlation with age in the bilateral DLPFC, right STG, bilateral insulae, bilateral caudate nuclei, left anterior cingulate gyrus, bilateral inferior parietal lobules, bilateral precunei, and bilateral fusiform gyri. (Bottom) The volume reduction associated with normal aging in each genotypic group ($p < 0.05$, FDR corrected). (Left) Results of individuals with homozygous Val-BDNF. Individuals with homozygous Val-BDNF showed negative correlation with age in the bilateral insulae (right: t-value: 4.36, TAL: 42, −2, 4; left: t-value: 4.52, TAL: −43, −2, 4) and the right superior temporal gyrus (t-value: 4.57, TAL: 47, 9, −4). (Right) Results of Met-BDNF carriers. The Met-BDNF carriers showed negative correlation with age in the bilateral dorsolateral prefrontal cortices (right: t-value: 6.5, TAL: 52, 21, 26; left: t-value: 6.12, TAL: −48, 19, 32) as well as the bilateral insulae and the superior temporal gyri.

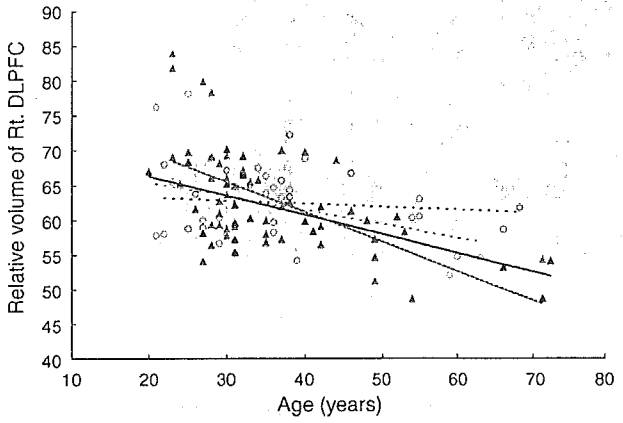

Fig. 3. Scatter plot of relative gray matter volume of the right DLPFC against age in each genomic group. The Met-BDNF carriers showed more significant volume reduction with normal aging compared to homozygous Val-BDNF subjects in the bilateral DLPFC in each gender (right: male Met-BDNF carriers: $y=-0.27x+71.8$, $r=-0.71$, $p<0.0001$, male homozygous Val-BDNF subjects: $y=-0.046x+64.2$, $r=-0.12$, $p=0.67$, female Met-BDNF carriers: $y=-0.43x+78.4$, $r=-0.56$, $p<0.001$, female homozygous Val-BDNF subjects: $y=-0.20x+69.5$, $r=-0.41$, $p=0.03$; left: male Met-BDNF carriers: $y=-0.20x+67.2$, $r=-0.53$, $p=0.01$, male homozygous Val-BDNF: $y=-0.11x+65.3$, $r=-0.25$, $p=0.367$, female Met-BDNF carriers: $y=-0.48x+77.0$, $r=-0.71$, $p<0.0001$, female homozygous Val-BDNF: $y=-0.14x+65.3$, $r=-0.27$, $p=0.18$). Due to limitations of space, only the plot at the right DLPFC in each gender is shown. Blue stands for male subjects and red stands for female subjects. Open circle: homozygous Val-BDNF; closed triangle: Met-BDNF carrier. Dotted lines are the regression line of homozygous Val-BDNF, whereas solid lines are those of Met-BDNF carrier.

reduction in the right inferior parietal lobules (BA40, t-value: 3.86, Talairach coordinates: 40, −43, 53). We found a significant interaction effect (male: $p=0.003$, female: $p<0.0001$) between the aging effect and the genotype on the gray matter volume in the DLPFC in each gender. (right: male Met-BDNF carriers: $r=-0.71$, $p<0.001$, male homozygous Val-BDNF subjects: $r=-0.12$, $p=0.67$; female Met-BDNF carriers: $r=-0.56$, $p<0.001$, female homozygous Val-BDNF subjects: $r=-0.41$, $p=0.03$; left: male Met-BDNF carriers: $r=-0.53$, $p=0.01$, male homozygous Val-BDNF subjects: $r=-0.25$, $p=0.367$, female Met-BDNF carriers: $r=-0.71$, $p<0.0001$, female homozygous Val-BDNF subjects: $r=-0.27$, $p=0.18$) (Fig. 3).

This is the first study which investigated the impacts of BDNF Val66Met polymorphism on age-associated brain morphological changes in normal individuals. We found an exaggerated age-related volume reduction of the DLPFC in the Met-BDNF carriers.

Several studies demonstrated morphological changes associated with normal aging in the STG, insula, inferior parietal lobules, motor cortex, ACC, and DLPFC [10,24]. In consistent with previous studies, our data also showed age-related volume reduction in similar regions in all subjects' analysis of each gender. Further analysis revealed that the Met-BDNF carriers showed a stronger negative correlation between age and gray matter volume in the DLPFC and right precentral gyrus when compared to individuals with homozygous Val-BDNF. Though the mechanisms underlying the predilection of the prefrontal cortex for age-related volume reduction are still unclear, the prefrontal cortex exhibits the greatest age-related alteration of GABA and glutamate [11], and glucose metabolism and age-related declines in regional cerebral blood flow [4]. Though there has been no study investigating the relationship between Val66Met SNP and vulnerability to age-related changes, BDNF protein itself is reported to be associated with aging. Amounts of BDNF protein in hippocampal pyramidal neurons and dentate granule cells are decreased during aging in monkeys [14]. Further, several studies demonstrated neuroprotective effects of BDNF [3,29]. Our data suggest that the Met-BDNF carriers, particularly females carrying Met-BDNF allele, may be more vulnerable to aging than individuals with homozygous Val-BDNF. Considering the fact that prefrontal cortex is one of the regions in which BDNF is expressed abundantly [25], we suggest that the Val66Met polymorphism may be associated with functional variances of neuroprotective and stress resistant effects of BDNF, which results in different effects on age-related morphological changes. Furthermore, we found a reduction of the striatal volumes in met-BDNF carriers as compared to individuals with homozygous Val-BDNF. It has been postulated that enhancement of BDNF in the cortex may be involved in protection of striatal neurons against damage via anterograde transport because BDNF exerts neuroprotective effects against excitoxicity in the striatum [1,16]. The result, reduced volumes in the striatum in met-BDNF carriers, may again suggest the reduced neuroprotective effects of met-BDNF. Since there has been no direct evidence of differential regulation of vulnerability to neurodegenerative process by BDNF Val66Met polymorphism, further study such as investigating how Val66Met SNP affects cell survival in a cellular model is required to clarify our speculation.

Although we could not replicate results of the previous studies, the smaller hippocampus in the Met-BDNF carriers [23,28], our data also suggest that BDNF polymorphism should have impacts on brain morphology associated with episodic memory. The discrepancy between our results and those of the previous studies could be partially explained by the racial difference. Binding its receptor TrkB, BDNF activates several pathways including the PI3-kinase/Akt, the mitogen-activated protein kinase, and PLC-gamma1 pathway [15]. These signals are known to be critical for survival of neuron, suggesting that not only Val66Met polymorphism of BDNF, but also interaction of polymorphism of each signal or molecule has effects on brain morphology. Racial differences might be related to such interactions, resulting in the different findings. This may partially contribute to the discrepancy in associations between BDNF polymorphism and the prevalence of neuropsychiatric diseases in Asian and Caucasian populations [17,27].

Finally, we mention a limitation of this study. To explore the association between aging effects on the brain morphology and the Val66Met polymorphism, we performed a cross-sectional study. There is a secular bias, which can be resolved by a longitudinal study. In this context, our data may be considered preliminary rather than conclusive. However, a recent longitudinal MR study of normal aging demonstrated that cross-sectional and longitudinal estimates of atrophy rates were similar [26].

In conclusion, we found that Val66Met polymorphism of BDNF had impacts on age-associated morphological changes in Japanese subjects. Our data suggest that Val66Met polymorphism of BDNF may play important roles for vulnerability to age-related morphological changes as well as the efficiency of plasticity, especially in DLPFC. Furthermore, we suggest that genotype effects of the BDNF gene on brain morphology might differ in female from in male.

Acknowledgements

The authors thank Ms. Tomoko Shizuno and Ms. Keiko Okada for technical assistance. This work was supported in part by Grants-in-Aid from the Japanese Ministry of Health, Labor and Welfare (H17-kokoro-007 and H16-kokoro-002), the Japanese Ministry of Education, Culture, Sports, Science and Technology, Core research for Evolutional Science and Technology (CREST) of Japan Science and Technology Agency (JST), Japan Foundation for Neuroscience and Mental Health, and the Program for Promotion of Fundamental Studies in Health Science of the Organization for Pharmaceuticals and Medical Devices Agency (PMDA).

References

[1] C.A. Altar, N. Cai, T. Bliven, M. Juhasz, J.M. Conner, A.L. Acheson, R.M. Lindsay, S.J. Wiegand, Anterograde transport of brain-derived neurotrophic factor and its role in the brain, Nature 389 (1997) 856–860.
[2] J. Ashburner, K.J. Friston, Voxel-based morphometry—the methods, Neuroimage 11 (2000) 805–821.
[3] Z.C. Baquet, J.A. Gorski, K.R. Jones, Early striatal dendrite deficits followed by neuron loss with advanced age in the absence of anterograde cortical brain-derived neurotrophic factor, J. Neurosci. 24 (2004) 4250–4258.
[4] M. Bentourkia, A. Bol, A. Ivanoiu, D. Labar, M. Sibomana, A. Coppens, C. Michel, G. Cosnard, A.G. De Volder, Comparison of regional cerebral blood flow and glucose metabolism in the normal brain: effect of aging, J. Neurol. Sci. 181 (2000) 19–28.
[5] C. Buchel, R.J. Wise, C.J. Mummery, J.B. Poline, K.J. Friston, Nonlinear regression in parametric activation studies, Neuroimage 4 (1996) 60–66.
[6] Z.Y. Chen, P.D. Patel, G. Sant, C.X. Meng, K.K. Teng, B.L. Hempstead, F.S. Lee, Variant brain-derived neurotrophic factor (BDNF) (Met66) alters the intracellular trafficking and activity-dependent secretion of wild-type BDNF in neurosecretory cells and cortical neurons, J. Neurosci. 24 (2004) 4401–4411.
[7] C.E. Coffey, J.F. Lucke, J.A. Saxton, G. Ratcliff, L.J. Unitas, B. Billig, R.N. Bryan, Sex differences in brain aging: a quantitative magnetic resonance imaging study, Arch. Neurol. 55 (1998) 169–179.
[8] M.F. Egan, M. Kojima, J.H. Callicott, T.E. Goldberg, B.S. Kolachana, A. Bertolino, E. Zaitsev, B. Gold, D. Goldman, M. Dean, B. Lu, D.R. Weinberger, The BDNF val66met polymorphism affects activity-dependent secretion of BDNF and human memory and hippocampal function, Cell 112 (2003) 257–269.
[9] C.R. Genovese, N.A. Lazar, T. Nichols, Thresholding of statistical maps in functional neuroimaging using the false discovery rate, Neuroimage 15 (2002) 870–878.
[10] C.D. Good, I.S. Johnsrude, J. Ashburner, R.N. Henson, K.J. Friston, R.S. Frackowiak, A voxel-based morphometric study of ageing in 465 normal adult human brains, Neuroimage 14 (2001) 21–36.
[11] I.D. Grachev, A. Swarnkar, N.M. Szeverenyi, T.S. Ramachandran, A.V. Apkarian, Aging alters the multichemical networking profile of the human brain: an in vivo (1)H-MRS study of young versus middle-aged subjects, J. Neurochem. 77 (2001) 292–303.
[12] A.R. Hariri, T.E. Goldberg, V.S. Mattay, B.S. Kolachana, J.H. Callicott, M.F. Egan, D.R. Weinberger, Brain-derived neurotrophic factor val66met polymorphism affects human memory-related hippocampal activity and predicts memory performance, J. Neurosci. 23 (2003) 6690–6694.
[13] R. Hashimoto, T. Okada, T. Kato, A. Kosuga, M. Tatsumi, K. Kamijima, H. Kunugi, The breakpoint cluster region gene on chromosome 22q11 is associated with bipolar disorder, Biol. Psychiatry 57 (2005) 1097–1102.
[14] M. Hayashi, F. Mistunaga, K. Ohira, K. Shimizu, Changes in BDNF-immunoreactive structures in the hippocampal formation of the aged macaque monkey, Brain Res. 918 (2001) 191–196.
[15] E.J. Huang, L.F. Reichardt, Neurotrophins: roles in neuronal development and function, Annu. Rev. Neurosci. 24 (2001) 677–736.
[16] Z. Kokaia, G. Andsberg, Q. Yan, O. Lindvall, Rapid alterations of BDNF protein levels in the rat brain after focal ischemia: evidence for increased synthesis and anterograde axonal transport, Exp. Neurol. 154 (1998) 289–301.
[17] H. Kunugi, Y. Iijima, M. Tatsumi, M. Yoshida, R. Hashimoto, T. Kato, K. Sakamoto, T. Fukunaga, T. Inada, T. Suzuki, N. Iwata, N. Ozaki, K. Yamada, T. Yoshikawa, No association between the Val66Met polymorphism of the brain-derived neurotrophic factor gene and bipolar disorder in a Japanese population: a multicenter study, Biol. Psychiatry 56 (2004) 376–378.
[18] E.A. Maguire, D.G. Gadian, I.S. Johnsrude, C.D. Good, J. Ashburner, R.S. Frackowiak, C.D. Frith, Navigation-related structural change in the hippocampi of taxi drivers, Proc. Natl. Acad. Sci. (2000) 4398–4403.
[19] J.A. Maldjian, P.J. Laurienti, R.A. Kraft, J.H. Burdette, An automated method for neuroanatomic and cytoarchitectonic atlas-based interrogation of fMRI data sets, Neuroimage 19 (2003) 1233–1239.
[20] K. Matsuoka, Y. Kim, H. Hiro, Y. Miyamoto, K. Fujita, K. Tanaka, K. Koyama, N. Kazuki, Development of Japanese Adult Reading Test (JART) for Predicting Premorbid IQ in Mild Dementia, Seishinigaku 44 (2002) 503–511.
[21] J.K. Morse, S.J. Wiegand, K. Anderson, Y. You, N. Cai, J. Carnahan, J. Miller, P.S. DiStefano, C.A. Altar, R.M. Lindsay, Brain-derived neurotrophic factor (BDNF) prevents the degeneration of medial septal cholinergic neurons following fimbria transection, J. Neurosci. 13 (1993) 4146–4156.
[22] H.E. Nelson, A. O'Connell, Dementia: the estimation of premorbid intelligence levels using the New Adult Reading Test, Cortex 14 (1974) 234–244.
[23] L. Pezawas, B.A. Verchinski, V.S. Mattay, J.H. Callicott, B.S. Kolachana, R.E. Straub, M.F. Egan, A. Meyer-Lindenberg, D.R. Weinberger, The brain-derived neurotrophic factor val66met polymorphism and variation in human cortical morphology, J. Neurosci. 24 (2004) 10099–10102.
[24] N. Raz, F. Gunning-Dixon, D. Head, K.M. Rodrigue, A. Williamson, J.D. Acker, Aging, sexual dimorphism, and hemispheric asymmetry of the cerebral cortex: replicability of regional differences in volume, Neurobiol. Aging 25 (2004) 377–396.
[25] M. Sandrini, S.F. Cappa, S. Rossi, P.M. Rossini, C. Miniussi, The role of prefrontal cortex in verbal episodic memory: rTMS evidence, J. Cogn. Neurosci. 15 (2003) 855–861.
[26] R.I. Scahill, C. Frost, R. Jenkins, J.L. Whitwell, M.N. Rossor, N.C. Fox, A longitudinal study of brain volume changes in normal aging using serial registered magnetic resonance imaging, Arch. Neurol. 60 (2003) 989–994.
[27] P. Sklar, S.B. Gabriel, M.G. McInnis, P. Bennett, Y.M. Lim, G. Tsan, S. Schaffner, G. Kirov, I. Jones, M. Owen, N. Craddock, J.R. DePaulo, E.S. Lander, Family-based association study of 76 candidate genes in bipolar disorder: BDNF is a potential risk locus. Brain-derived neutrophic factor, Mol. Psychiatry 7 (2002) 579–593.
[28] P.R. Szeszko, R. Lipsky, C. Mentschel, D. Robinson, H. Gunduz-Bruce, S. Sevy, M. Ashtari, B. Napolitano, R.M. Bilder, J.M. Kane, D. Goldman, A.K. Malhotra, Brain-derived neurotrophic factor val66met polymorphism and volume of the hippocampal formation, Mol. Psychiatry 10 (2005) 631–636.
[29] H. Yanamoto, I. Nagata, M. Sakata, Z. Zhang, N. Tohnai, H. Sakai, H. Kikuchi, Infarct tolerance induced by intra-cerebral infusion of recombinant brain-derived neurotrophic factor, Brain Res. 859 (2000) 240–248.

The Breakpoint Cluster Region Gene on Chromosome 22q11 Is Associated with Bipolar Disorder

Ryota Hashimoto, Takeya Okada, Tadafumi Kato, Asako Kosuga, Masahiko Tatsumi, Kunitoshi Kamijima, and Hiroshi Kunugi

Background: *Although the pathogenesis of bipolar disorder remains unclear, heritable factors have been shown to be involved. The breakpoint cluster region (BCR) gene is located on chromosome 22q11, one of the most significant susceptibility loci in bipolar disorder linkage studies. The BCR gene encodes a Rho GTPase activating protein, which is known to play important roles in neurite growth and axonal guidance.*

Methods: *We examined patients with bipolar disorder (n = 171), major depressive disorder (n = 329) and controls (n = 351) in Japanese ethnicity for genetic association using eleven single nucleotide polymorphisms (SNPs), including a missense one (A2387G; N796S), in the genomic region of BCR.*

Results: *Significant allelic associations with bipolar disorder were observed for three SNPs, and associations with bipolar II disorder were observed in ten SNPs including N796S SNP (bipolar disorder, p = .0054; bipolar II disorder p = .0014). There was a significant association with major depression in six SNPs. S796 allele carriers were in excess in bipolar II patients (p = .0046, odds ratio = 3.1, 95% CI 1.53–8.76). Furthermore, we found a stronger evidence for association with bipolar II disorder in a multi-marker haplotype analysis (p = .0002).*

Conclusions: *Our results suggest that genetic variations in the BCR gene could confer susceptibility to bipolar disorder and major depressive disorder.*

Key Words: Breakpoint cluster region (BCR), bipolar disorder, major depression, 22q, association study, single nucleotide polymorphism (SNP)

Bipolar disorder is a major psychiatric disorder that is characterized by fluctuation between abnormal mood states of mania and depression. Since lithium has been one of the primary drugs used to treat bipolar disorder, molecular and cellular actions of this drug are believed to be clues of the pathophysiology of this disease, e.g. inhibition of glycogen synthase kinase-3, inositol monophosphatase, or N-methyl-D-aspartate (NMDA) receptor activity, activation of BDNF/Trk pathway, and enhancement of neurogenesis and neuronal progenitor proliferation (Chen et al 2000; Hallcher and Sherman 1980; Hashimoto et al 2002a, 2002b, 2003; Klein and Melton 1996). Recently, a common mechanism of action for three mood-stabilizing drugs, lithium, valproate and carbamazepine, has been identified (Williams et al 2002). These drugs inhibit the collapse of sensory neuron growth cones and increase growth cone area. Inositol reverses the effects of the drugs on growth cones, implicating inositol depletion in their action.

The breakpoint cluster region (BCR) gene is located on chromosome 22q, one of the most consistently replicated susceptibility loci in linkage studies of bipolar disorder (Detera-Wadleigh et al 1999; Edenberg et al 1997; Kelsoe et al 2001; Turecki et al 2001). A recent meta-analysis of eleven published genome scans for bipolar disorder revealed the strongest evidence for susceptibility loci on 22q and 13q (Badner and Gershon 2002). The BCR gene encodes a Rho GTPase-activating protein (GAP) highly expressed in hippocampal pyramidal cell layer and dentate gyrus (Fioretos et al 1995). The Rho family of GTP binding proteins acts as a key regulator for developing neuronal network, e.g. growth cone and neurite formation (Negishi and Katoh 2002). These proteins cycle between active GTP-bound and inactive GDP-bound forms. The activation of GTP-bound form is regulated by GAPs, which stimulate GTP hydrolysis, leading to inactivation (Etienne-Manneville and Hall 2002).

Therefore, genetic variability of the BCR gene is of considerable interest in the evaluation of risk of bipolar disorder. To our knowledge, however, there is no study examining the possible association between the BCR gene and bipolar disorder. The BCR gene (Online Mendelian Inheritance in Man [OMIM]:151410) consists of 23 exons and 22 introns, spanning 135 Kb. We searched for polymorphisms in the BCR gene in silico and selected eleven single nucleotide polymorphisms (SNPs), including a common single nucleotide substitution (A2387G; National Center for Biotechnology Information [NCBI] SNP ID: rs140504) in exon 10 giving rise to an amino acid change of asparagine to serine at codon 796 (N796S; NCBI Protein ID: NP_004318). In the present study, we performed an association study with SNPs in the region of the BCR gene in a Japanese population of bipolar and major depression cases and controls.

Methods and Materials

Subjects

Subjects were 171 patients with bipolar disorder (65 males and 106 females with mean age of 50.8 years [SD 14.9] and mean age of onset of 39.2 years [SD 15.2], 102 bipolar I [43 males and 59 females] and 69 bipolar II patients [22 males and 47 females]), 329 patients with major depressive disorder (116 males and 213 females with mean age of 54.3 years [SD 16.0] and mean age of onset of 46.7 years [SD 15.3]) and 351 healthy controls (170 males

From the Department of Mental Disorder Research (RH, TO, HK), National Institute of Neuroscience, National Center of Neurology and Psychiatry, Kodaira; Showa University Karasuyama Hospital (AK); Department of Psychiatry (MT, KK), Showa University School of Medicine, Tokyo; Laboratory for Molecular Dynamics of Mental Disorders (TK), RIKEN Brain Science Institute, Wako, Saitama; Yokohama Shinryo Clinic (MT), Yokohama, Kanagawa, Japan.

Address reprint requests to Ryota Hashimoto M.D., Ph.D., Department of Mental Disorder Research, National Institute of Neuroscience, National Center of Neurology and Psychiatry, 4-1-1, Ogawahigashicho, Kodaira, Tokyo, 187-8502, Japan; E-mail: rhashimo@ncnp.go.jp.

Received August 5, 2004; revised February 2, 2005; accepted February 14, 2005.

0006-3223/05/$30.00
doi:10.1016/j.biopsych.2005.02.019

BIOL PSYCHIATRY 2005;57:1097–1102

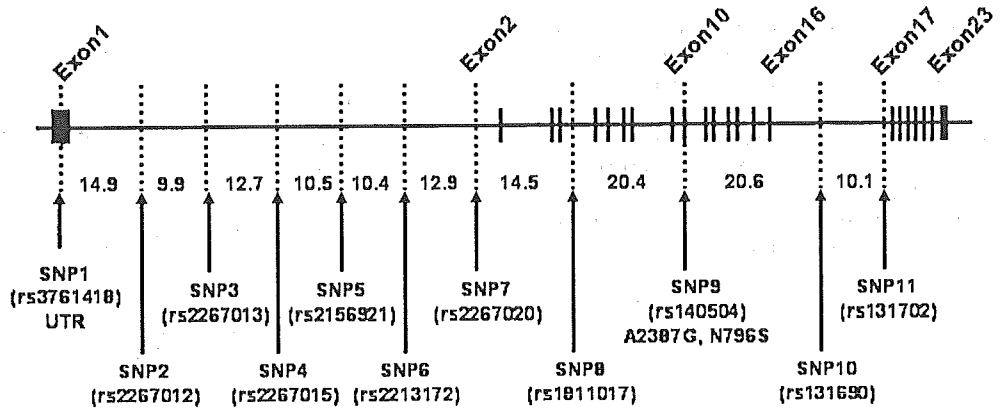

Figure 1. Genomic structure and location of single nucleotide polymorphisms (SNPs) for human Breakpoint Cluster Region (*BCR*) gene. Exons are denoted by bold vertical lines in black. The rs number of each SNP is the National Center for Biotechnology Information SNP cluster ID from the dbSNP database. The distances of the adjunct SNPs (Kb) are also shown.

and 181 females with mean age of 40.2 years [SD 12.0]). In addition, subjects who were examined in our previous study on the XBP1 gene (Kakiuchi et al 2003), were included in this study; 83 patients with bipolar disorder (27 males and 56 females with mean age of 48.1 years [SD 14.6] and mean age of onset of 35.9 years [SD 15.1], 57 bipolar I [23 males and 34 females] and 26 bipolar II patients [4 males and 22 females]) and 97 healthy controls (51 males and 46 females with mean age of 38.8 years [SD 13.4]). All the subjects were biologically unrelated Japanese. Consensus diagnosis was made for each patient by at least two trained psychiatrists according to the DSM-IV criteria, based on all available information, including clinical interview, medical records and other research assessments. Controls were healthy volunteers who had no current or past contact to psychiatric services. Subjects with significant medical problems, history of head trauma, neurosurgery and alcohol or substance abuse were excluded. After description of the study, written informed consent was obtained from every subject. The study protocol was approved by institutional ethical committees (Showa University School of Medicine, RIKEN Brain Science Institute and National Center of Neurology and Psychiatry, Tokyo, Japan).

SNP Genotyping

Venous blood was drawn from the subjects and genomic DNA was extracted from whole blood according to the standard procedures. Eleven SNPs (SNP1: rs3761418, SNP2: rs2267012, SNP3: rs2267013, SNP4: rs2267015, SNP5: rs2156921, SNP6: rs2213172, SNP7: rs2267020, SNP8: rs1811017, SNP9: rs140504, SNP10: rs131690, SNP11: rs131702; see figure 1) in the BCR gene were genotyped using the TaqMan 5'-exonuclease allelic discrimination assay, described previously (Hashimoto et al 2004; Hashimoto et al 2005). Briefly, primers and probes for detection of the SNPs are: SNP1: forward primer 5'-GGGAGTGAAACAAAATCTTTGATGGTT-3', reverse primer 5'-ATCAGACTCCCTGCTCTTTGC-3', probe 1 5'-VIC-CTGTCTCAGATTTCCAGMGB-3', and probe 2 5'-FAM-CTGTCTCAGATCTCCAG-MGB-3'; SNP2: forward primer 5'-GCATTTTGCAGAATGTCTTCTCTCA-3', reverse primer 5'-ACACTCAGCTAAGAGGGTTCCT-3', probe 1 5'-VIC-CCCTGTGAAGGAGTG-MGB-3', and probe 2 5'-FAMCCTGTGGAGGAGTG-MGB-3'; SNP3: forward primer 5'-TCTTTGTCAGCGCTGTGGTT-3', reverse primer 5'- CCCACAACAGCAATAAACTAGCAAA-3', probe 1 5'-VIC- CAGTAAGTTCTTTCCCTACCAAG-MGB-3', and probe 2 5'-FAM- TAAGTTCTTTCCCCACCAAG-MGB-3'; SNP4: forward primer 5'-CCACCCTAGGGCATTTTCCT-3', reverse primer 5'-CCAGCTTTCCACTGTTATGAATACAATG-3', probe 1 5'-VIC-CCCCTTTTCTTTTATGGTAG-MGB-3', and probe 2 5'-FAM-CCCCTTTTCTTTTTTGGTAGMGB-3'; SNP5: forward primer 5'-GGAATAGCAGAGTATCTTTTCAACTAGGTT-3', reverse primer 5'-GGACTTCTGGCCCCTTTCAG-3', probe 1 5'-VIC-CCCCTCAATTGCAC-MGB-3', and probe 2 5'-FAM-CCCCTCAGTTGCAC-MGB-3'; SNP6: forward primer 5'-CTAGCAGCTGTGCTCATGGA-3', reverse primer 5'-AGGCCCAGCTCCTATCCT-3', probe 1 5'-VIC-ATCTCACGTCCTCCC-MGB-3', and probe 2 5'-FAM-AATCTCACCTCCTCCCMGB-3'; SNP7: forward primer 5'-CTCGGTGTTGACTTGACCTTACA-3', reverse primer 5'-GGTGGAGCACCTTTTATCTGAGT-3', probe 1 5'-VIC-CTTTCCGAGCCCATG-MGB-3', and probe 2 5'-TTTCCGCGCCCATG-MGB-3'; SNP8: forward primer 5'-GCCACTTCCTGGAAAGAAAGGT-3', reverse primer 5'-TGAGGTCTGGCTGGTGCTA-3', probe 1 5'-VIC-CTGCCAATAGCCC-MGB-3', and probe 2 5'-CTGCCAGTAGCCC-MGB-3'; SNP9: forward primer 5'-AGCTGGACGCTTTGAAGATCA-3', reverse primer 5'-TGGTGTGCACCTTCTCTCTCT-3', probe 1 5'-VIC-CCAGATCAAGAATGACAT-MGB-3', and probe 2 5'-FAM-CCAGATCAAGAGTGACAT-MGB-3'; SNP10: forward primer 5'-CCTGCCTGCCCAGTCC-3', reverse primer 5'-CCCTGGGTTGCAAGGTCTT-3', probe 1 5'-VIC-CAGGCATATTCCTCA-MGB-3', and probe 2 5'-FAMCAGGCATGTTCCTCA-MGB-3'; SNP11: forward primer 5'-CAGACTGTGTTCGGGTGACA-3', reverse primer 5'-ACCCGGCACTATCCAGACA-3', probe 1 5'-VIC-CAGGAGCTTGTCCTTAAMGB-3', and probe 2 5'-FAM-CAGGAGCTTGTCATTAA-MGB-3'. PCR cycling conditions were: at 95°C for 10 min, 45 cycles of 92°C for 15 sec and 60°C for 1 min.

Statistical Analysis

Statistical analysis of association studies was performed using SNPAlyse software (DYNACOM, Yokohama, Japan). The presence of Hardy-Weinberg equilibrium was examined using the χ^2 test for goodness of fit. Allele distributions between patients and controls were analyzed by the χ^2 test for independence. The measures of linkage disequilibrium (LD), denoted as D' and r^2, were calculated from the haplotype frequency using Expectation-Maximization algorithm. Case-control haplotype analysis was performed by the permutation method to obtain empirical significance (Good 2000). The global p-values represent the overall significance using the χ^2 test when the observed versus expected frequencies of all the haplotypes are considered together. The individual haplotypes were tested for association by

grouping all others together and applying the χ^2 test with 1 *df*. Calculations of *p*-values were based on 10,000 replications. All p-values reported are two tailed. Statistical significance was defined at $p < .05$.

The population homogeneity was assessed using STRUCTURE software (http://pritch.bsd.uchicago.edu/software.html) (Pritchard et al 2000) with eight SNPs, as described previously (Yamada et al 2004). In the application of the Markov chain Monte Carlo method, 1,000,000 replications were used for the burn-in period of the chain and for parameter estimation. Analysis was run at K = 1, 2, 3, 4, and 5. From these results, best estimate of K was found by calculating posterior probabilities, Pr (K = 1, 2, 3, 4, or 5).

Results

The genotype distributions of all the eleven SNPs were in Hardy-Weinberg equilibrium for both the controls and patients with bipolar disorder and major depressive disorder (data not shown). Allele frequencies of the eleven SNPs among the patients and controls are shown in Table 1. The minor alleles of SNP9, SNP10 and SNP11 were in excess in our total bipolar patients when compared to controls (SNP9: $\chi^2 = 7.73$, $df = 1$, $p = .0054$, odds ratio = 1.45 95% CI 1.11–1.84; SNP10: $\chi^2 = 7.48$, $df = 1$, $p = .0063$, odds ratio = 1.50 95% CI 1.14–2.03; SNP11: $\chi^2 = 9.05$, $df = 1$, $p = .0026$, odds ratio = 1.49 95% CI 1.15–1.93), while significant association of the other eight SNPs was not observed with the overall bipolar patients (Table 1). When we examined bipolar I and II separately, there were significant differences in the allele frequency for ten SNPs between patients with bipolar II disorder and controls, while there was a significant difference for one SNP between those with bipolar I disorder and controls (Table I). Then, we examined a possible association between major depression and the BCR gene. A significant difference in the allele frequency was found for six SNPs between patients with major depressive disorder and controls, and for seven SNPs between total patients with mood disorders and controls (Table I).

We then focused on the association between the SNPs in the BCR gene and bipolar II disorder. The frequencies of minor allele carriers of the eleven SNPs were compared with major allele homozygotes, as we assumed that minor alleles might have a dominant effect for developing the disease. Nine out of eleven SNPs were significantly associated with bipolar II disorder (Table 2). The smallest *p*-value was obtained in SNP9, N796S missense polymorphism. The S796 allele was significantly more frequent in the bipolar II patients when compared to the controls ($\chi^2 = 8.58$, $df = 1$, $p = .0046$, odds ratio = 3.1, 95% CI 1.53–8.76).

To further analyze the haplotype structure in Japanese population, we computed *D'* and r^2 values for all combinations of the eleven SNPs spanning the BCR locus at an average density of 12.3kb (Table 3). Forty-nine of 55 of possible 2-marker haplotype analysis for all combinations of the eleven SNPs yielded globally significant evidence for association ($p < .05$). That high population of the associated haplotypes is not surprising given the nonindependence of the markers, suggesting that Bonferroni correction might not be appropriate. Adjacent combinations of up to ten markers were examined for association with bipolar II disorder. Six of the nine possible 3-marker haplotype revealed significant evidence for association, as did six of eight of the 4-marker haplotypes and four of seven of 5-marker haplotypes. In total, more than 70% of all possible haplotypes showed the results that gave global significance at $p < .05$. Notably, all the possible combinations of haplotypes including SNP9 (N796S) were associated with bipolar disorder.

Table 1. Allele Distributions for 11 SNPs in the BCR Gene Among Patients With Bipolar Disorder and With Major Depression and Controls

		Controls	BP			BPI			BPII			MDD			Total cases		
SNP-ID	SNP	*n* = 351	*n* = 171	*p* Value	OR	*n* = 102	*p* Value	OR	*n* = 69	*p* Value	OR	*n* = 329	*p* Value	OR	*n* = 500	*p* Value	OR
SNP1	A/G	.349	.395	ns	—	.343	ns	—	.471	.0066	1.66	.415	.012	1.32	.408	.014	1.29
SNP2	A/G	.405	.456	ns	—	.402	ns	—	.536	.0042	1.70	.474	.0097	1.33	.468	.0095	1.29
SNP3	A/G	.261	.295	ns	—	.230	ns	—	.391	.0018	1.82	.310	.044	1.27	.305	.047	1.24
SNP4	T/A	.289	.319	ns	—	.245	ns	—	.428	.0013	1.84	.347	.023	1.30	.337	.037	1.25
SNP5	A/G	.292	.319	ns	—	.245	ns	—	.428	.0017	1.81	.347	.031	1.29	.337	.050	1.23
SNP6	G/C	.298	.330	ns	—	.255	ns	—	.442	.0009	1.87	.353	.031	1.28	.345	.040	1.24
SNP7	G/T	.423	.477	ns	—	.436	ns	—	.536	.0144	1.58	.438	ns	—	.451	ns	—
SNP8	A/G	.051	.061	ns	—	.064	ns	—	.058	ns	—	.061	ns	—	.061	ns	—
SNP9	A/G	.481	.573	.0054	1.45	.534	ns	—	.630	.0014	1.84	.523	ns	—	.540	.018	1.26
SNP10	A/G	.218	.295	.0062	1.50	.270	ns	—	.333	.0036	1.79	.236	ns	—	.256	ns	—
SNP11	T/G	.393	.491	.0026	1.49	.480	.026	1.43	.507	.013	1.59	.386	ns	—	.422	ns	—

Minor allele frequencies in controls are shown. OR, odds ratio; BP, bipolar disorder; MDD, Major depressive disorder; SNP, single nucleotide polymorphism; BCR, breakpoint cluster region.

Table 2. Genotype Distributions for the SNPs in the BCR Gene Among the Patients With Bipolar II and Controls

	Controls			BPII			2/2 and 1/2 vs. 1/1	
SNP-ID	1/1	1/2	2/2	1/1	1/2	2/2	*p* Value	OR (95% CI)
SNP1	151 (43.0%)	155 (44.2%)	45 (12.8%)	19 (27.5%)	35 (50.7%)	15 (21.7%)	.017	1.99 (1.16–3.84)
SNP2	123 (35.0%)	172 (49.0%)	56 (16.0%)	15 (21.7%)	34 (49.3%)	20 (29.0%)	.031	1.94 (1.10–3.78)
SNP3	190 (54.1%)	139 (39.6%)	22 (6.3%)	26 (37.7%)	32 (46.4%)	11 (15.9%)	.012	1.95 (1.19–3.49)
SNP4	171 (48.7%)	157 (44.7%)	23 (6.6%)	22 (31.9%)	35 (50.7%)	12 (17.4%)	.010	2.03 (1.19–3.61)
SNP5	170 (48.4%)	157 (44.8%)	24 (6.8%)	22 (31.9%)	35 (50.7%)	12 (17.4%)	.012	2.01 (1.13–3.65)
SNP6	165 (47.0%)	163 (46.4%)	23 (6.6%)	21 (30.4%)	35 (50.7%)	13 (18.8%)	.011	2.03 (1.19–3.61)
SNP7	115 (32.8%)	175 (49.9%)	61 (17.4%)	15 (21.7%)	34 (49.3%)	20 (29.0%)	.070	1.75 (1.01–3.62)
SNP8	315 (89.7%)	36 (10.3%)	0 (0%)	61 (88.4%)	8 (11.6%)	0 (0%)	ns	—
SNP9	91 (25.9%)	182 (51.9%)	78 (22.2%)	7 (10.1%)	37 (53.6%)	25 (36.2%)	.0046	3.10 (1.53–8.76)
SNP10	215 (61.3%)	119 (33.9%)	17 (4.8%)	32 (46.4%)	28 (40.6%)	9 (13.0%)	.022	1.83 (1.08–3.19)
SNP11	128 (36.5%)	170 (48.4%)	53 (15.1%)	15 (21.7%)	38 (55.1%)	16 (23.2%)	.018	2.07 (1.20–4.02)

Allele 1 represents a major allele in each SNP. SNP, single nucleotide polymorphism; BCR, breakpoint cluster region; BP, bipolar disorder; OR, odds ratio.

Adjacent marker combinations yielding global evidence for association at $p < .005$ are presented in figure 2. The haplotypes that yielded global evidence for significant association at this level included the SNP9 and SNP10. The haplotypes that yielded the strongest global evidence for significant association consisted of markers SNP8-SNP9-SNP10-SNP11 (global permutation p value = .00041, 100,000 simulations). Given this result, we tested the contribution of individual haplotypes to the global result. The lowest p-value was obtained for the difference in the frequency of 1-2-2-2 haplotype (SNP8-SNP9-SNP10-SNP11), which was enriched in patients with bipolar II disorder compared with controls (estimated frequencies: patients 30.2% vs controls 16.7%, permutation p value = .0002). Another individual haplotype that yielded the evidence for significant association was 1-1-1-1 haplotype, which occurs at a frequency of 33.5% in the patients and 45.7% in the controls (permutation p value = .0066).

Discussion

We found a significant association between genetic variations of the BCR gene and bipolar disorder and major depressive disorder in a Japanese population. Our data suggest that the BCR gene is associated with bipolar II rather than bipolar I disorder. The weaker association with major depression compared to bipolar II disorder might be due to some patients with major depression who could develop bipolar II disorder in the future and/or the susceptibility both for bipolar II and major depression. The diagnostic category of bipolar II disorder is defined as less severe manic symptoms compared with bipolar I disorder. Bipolar II patients tend to have more previous episodes, including both depressive and hypo-manic, but less hospitalization and psychotic symptoms (Vieta et al 1997). Some studies showed that bipolar disorder is likely to be a quantitative trait (bipolar I – bipolar II – major depression), while other studies argued that bipolar II may be genetically distinct to bipolar I disorder (Kelsoe 2003). Bipolar I and bipolar II were of approximately similar prevalence in the first degree relatives of bipolar I probands (8.5 vs. 6.1%, respectively), while bipolar II was significantly more prevalent among the first degree relatives of bipolar II probands (3% vs. 30%, respectively) (Coryell et al 1984). These data suggest that some genes confer susceptibility to both bipolar I and bipolar II, while a separate and more common set of genes predisposes preferentially or exclusively to bipolar II disorder. Kelsoe proposed a model of bipolar genetics that some of the genes involved are specific for each of the phenotypes considered bipolar I, bipolar II and major depression and others are less specific and may predispose individuals to either bipolar disorders or major depression (Kelsoe 2003).

The XBP1 gene, which has been reported to be associated with bipolar disorder, is also located on the chromosome 22q (Kakiuchi et al 2003). However, the physical distance between the XBP1 and BCR gene is approximately 5.5 Mb, and the D' value between the -116C/G polymorphism of the XBP1 gene and

Table 3. Marker-to-Marker LD for All the Combinations of the 11 SNPs in the BCR Gene

—	SNP1	SNP2	SNP3	SNP4	SNP5	SNP6	SNP7	SNP8	SNP9	SNP10	SNP11
SNP1	—	.766[a]	.610[a]	.483[a]	.493[a]	.480[a]	.311[a]	.000	.240[b]	.002[b]	.067[a]
SNP2	.985[a]	—	.475[a]	.576[a]	.585[a]	.557[a]	.360[a]	.001	.279[a]	.009[b]	.081[a]
SNP3	.963[a]	.957[a]	—	.785[a]	.801[a]	.765[a]	.148[a]	.001	.114[b]	.026[a]	.015[a]
SNP4	.797[a]	.981[a]	.952[a]	—	.986[a]	.946[a]	.192[a]	.001[b]	.154[b]	.041[a]	.018[b]
SNP5	.800[a]	.981[a]	.968[a]	1.000[a]	—	.959[b]	.191[a]	.001[b]	.152[b]	.039[a]	.018[a]
SNP6	.779[a]	.945[a]	.959[a]	.993[a]	.993[b]	—	.193[a]	.001[a]	.153[b]	.040[a]	.016[b]
SNP7	.653[a]	.624[a]	.554[a]	.588[a]	.582[a]	.578[a]	—	.040[a]	.693[a]	.113[a]	.360
SNP8	.095	.137	.089	.086[b]	.078[b]	.106[a]	1.000[a]	—	.058[a]	.000	.006
SNP9	.644[b]	.617[a]	.549[b]	.593[b]	.585[b]	.579[b]	.937[a]	1.000[a]	—	.118[a]	.344[b]
SNP10	.064[b]	.147[b]	.183[a]	.244[a]	.241[a]	.247[a]	.546[a]	.105	.627[a]	—	.430[a]
SNP11	.285[a]	.291[a]	.165[a]	.169[b]	.170[a]	.154[b]	.638	.424	.702[b]	1.000[a]	—

For each pair of markers, the standardized D' is shown below the diagonal, and r^2 above the diagonal.
LD, linkage disequilibrium; SNP, single nucleotide polymorphism; BCR, breakpoint cluster region.
[a] $p < .05$.
[b] $p < .01$.

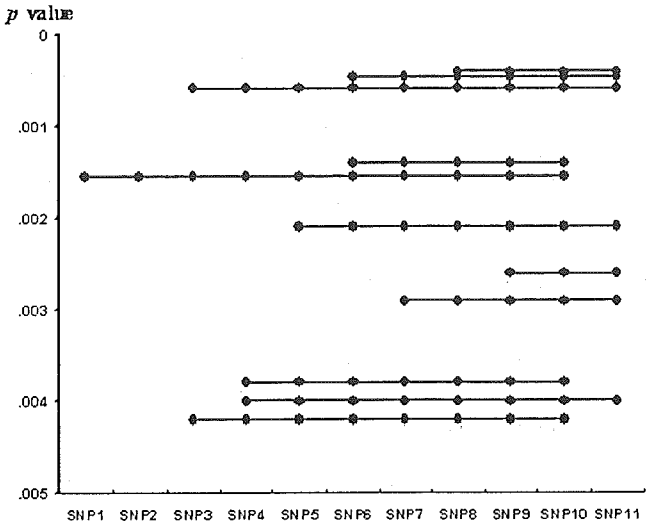

Figure 2. Plot of haplotypes showing global association to bipolar II disorder ($p < .005$). The x-axis scale is nonlinear in order to allow easy visualization of the different haplotypes. SNP, single nucleotide polymorphism.

any SNPs in the BCR gene is less than .3, and r^2 values are less than .004 both in patients and controls groups, suggesting that genetic association between bipolar disorder and both genes might be independent. In addition, we did not observe the evidence for the association between the -116C/G SNP and bipolar disorder in the population of the present study, although approximately half of the subjects in this study were overlapped with the Kakiuchi's study (G allele frequencies, Kakiuchi's, case: .71, control: .64; present study, case: .68, control: .70) (Kakiuchi et al 2003).

Our data suggest the existence in our sample of a risk haplotype and a protective haplotype consisting of SNP8-SNP9-SNP10-SNP11. We intended to determine the haplotype block structure of the region (Gabriel et al 2002), examining eleven SNPs at an average density of 12.3kb across the BCR gene. Unfortunately, we were not able to define the obvious haplotype blocks in a Japanese sample, because of the complex results of marker to marker LD. It is of interest how genetic variation might affect BCR function/expression. Although we have no evidence whether any of the SNPs in our haplotypes are functional, SNP9 associated with bipolar disorder might be functional as this SNP gives rise to an amino acid substitution of N796S in the functional domain, pleckstrin homology (PH) domain, of the BCR protein. This SNP might account for the susceptibility for bipolar disorder, as the individuals carrying the S796 allele were most significantly in excess in bipolar II patients in our study ($p = .0046$, odds ratio = 3.1). Alternatively, an unknown functional polymorphism, which is in LD with the SNPs and/or haplotypes, may be responsible for biologic susceptibility for bipolar II. Further work, e.g. dense mapping in the BCR gene, and functional analysis of N796S missense polymorphism, will be required to resolve this issue.

The function of the normal BCR gene product remains unclear, although the BCR-ABL fusion protein, which causes certain human leukemias, has been extensively studied (Pane et al 2002). The BCR gene encodes a 1271 amino acid protein containing several functional domains: a serine/threonine protein kinase domain, a Dbl homology domain, a PH domain and a Rho GTPase-activating protein domain. This protein acts as a serine/threonine kinase, a GTPase-activating protein for p21rac, and a Rho GTPase guanine nucleotide exchange factor (Diekmann et al 1991; Korus et al 2002; Maru and Witte 1991). The PH domain is a 100–120 amino acid protein module best known for its ability to bind phosphatidylinositol (Lemmon et al 2002). PH domain-containing proteins specifically recognize 3-phosphorylated phosphatidylinositol, allowing them to drive membrane recruitment in response to phosphatidylinositol 3-kinase activation. A dysfunction in the phosphatidylinositol signal transduction pathway appears to be implicated in the pathophysiology of bipolar disorder, e.g. increased intracellular calcium responsiveness and protein kinase C activity in platelets and transformed lymphoblasts, and decreased inositol levels in frontal cortex of the postmortem brain (Shimon et al 1997; Soares and Mallinger 1997). The N796S missense polymorphism in the PH domain of BCR could affect its binding activity to phosphatidylinositol, and then alter the phosphatidylinositol signal transduction pathway. Both asparagine and serine residue are neutral amino acids (polar amino acids), while only serine residue could be phosphorylated. Additionally, the sequence around N796 is evolutionarily conserved across several species, including fruit fly, African clawed frog, mouse, rat, and human. As S796 is unique for humans, this polymorphism might be associated with the higher brain function in humans.

As a common action of mood stabilizers is to inhibit the collapse of neuronal growth cone via depletion of inositol (Williams et al 2002), neuronal growth cone formation is likely to be involved in the pathogenesis of bipolar disorder. BCR is a RhoGAP protein, which inactivates the Rho GTPase. Rho GTPase proteins activate their effecters, which control cytoskeletal organization (Kaibuchi et al 1999), leading to the motile behavior of the neurite and growth cone (Huber et al 2003). As Rho associated kinase, one of the Rho effectors, regulates the dynamic reorganization of cytoskeletal proteins, such as actin, neurofilament and glial fibrillary acidic protein (Amano et al 1997; Hashimoto et al 1998; Kosako et al 1997), it is worth investigating the possible effect of BCR, including N796S amino acid change, on the growth cone formation and Rho associated kinase.

We have firstly demonstrated the possible association between the BCR gene and bipolar disorder in a Japanese population. The limitation of this work is that there were differences with regard to mean age and gender distribution between patients and controls. Thus, we assessed the population homogeneity and did not detect any evidence for such stratification in our samples with a Pr (K = 1) > .99. However, a false-positive association due to the small sample size of the bipolar II disorder patients could not be excluded in our study. Further investigations are warranted to confirm our findings in other samples.

We thank Tomoko Shizuno and Reiko Fujita for technical assistance and Dr. Kazuo Yamada and Kozo Kaibuchi for helpful discussions.

This work was supported by Grants-in-Aid from the Japanese Ministry of Health, Labor and Welfare, the Japanese Ministry of Education, Culture, Sports, Science and Technology, the Uehara Memorial Foundation, and Japan Foundation for Neuroscience and Mental Health.

Amano M, Chihara K, Kimura K, Fukata Y, Nakamura N, Matsuura Y, et al (1997): Formation of actin stress fibers and focal adhesions enhanced by Rho-kinase. *Science* 275:1308–1311.

Badner JA, Gershon ES (2002): Meta-analysis of whole-genome linkage scans of bipolar disorder and schizophrenia. *Mol Psychiatry* 7:405–411.

Chen G, Rajkowska G, Du F, Seraji-Bozorgzad N, Manji HK (2000): Enhancement of hippocampal neurogenesis by lithium. *J Neurochem* 75:1729–1734.